Supplementary Information

Analysis of mammalian gene function through broad-based phenotypic screens across a consortium of mouse clinics

The EUMODIC Consortium

I Supplementary Figures

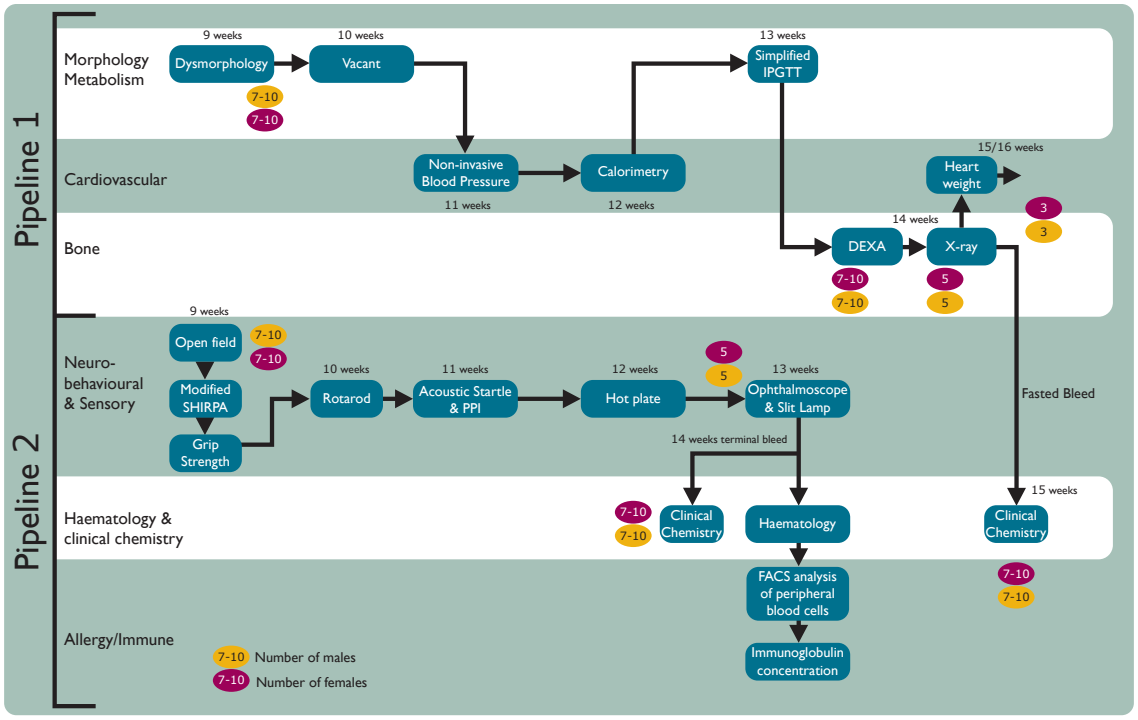

Supplementary Figure 1: EMPReSSlim Pipeline. EMPReSSslim comprises two phenotyping pipelines, covering a diverse set of biological and disease areas as indicated. In total 20 phenotyping tests are incorporated in the two pipelines. Note that a minimum cohort of 7 males and 7 females enters each pipeline.

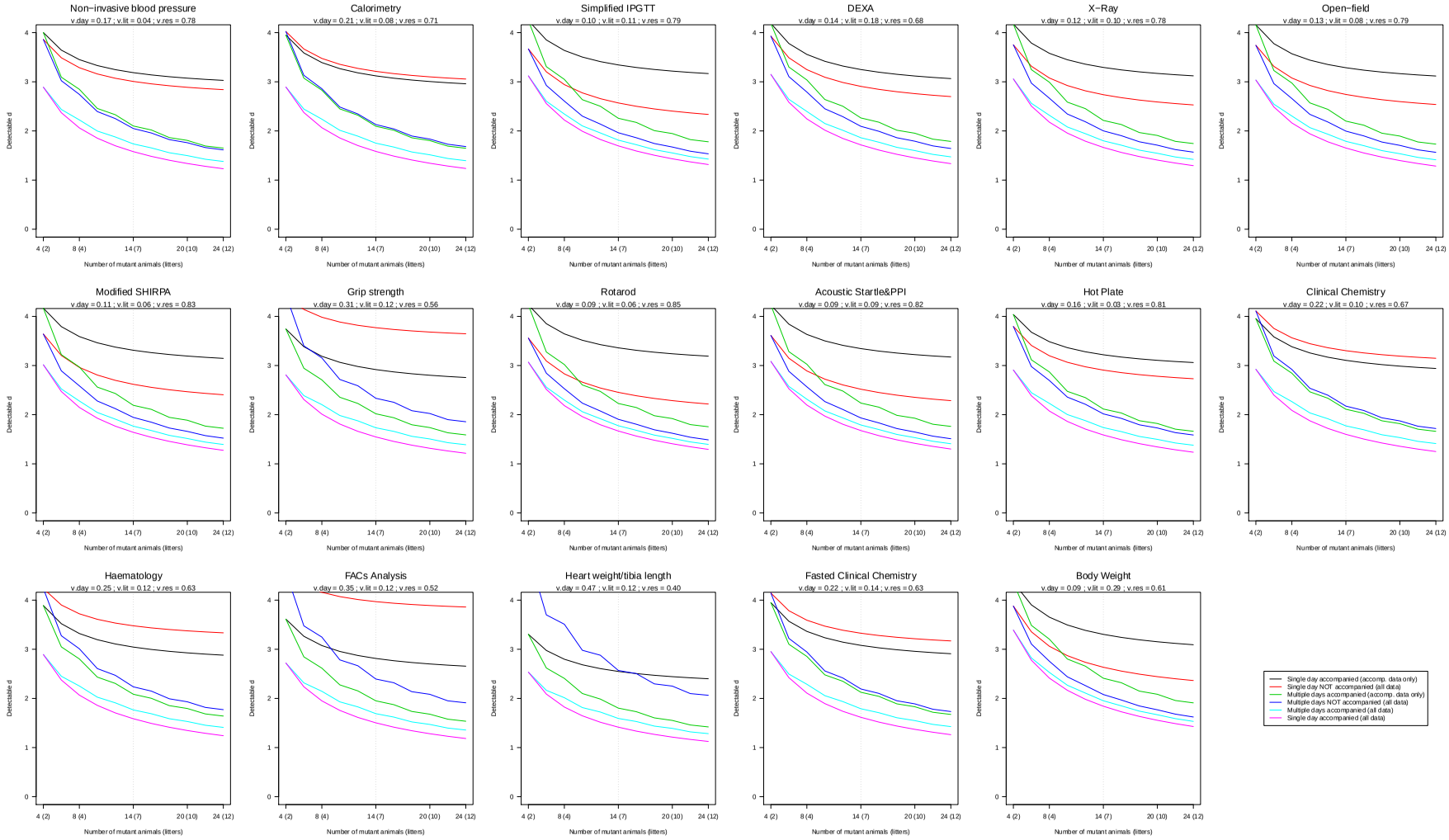

Supplementary Figure 2: Procedure-specific detectable standardized effect size Procedure-specific detectable standardized effect size, *d*, as a function of sample size, under a variety of experimental workflows and analysis approaches (identified in legend). The two qualitative design choices under consideration were: whether mutant animals were phenotyped across multiple days with four animals per day, or all on a single day; and whether baseline animals were phenotyped on the same day(s) as mutants (i.e. whether the mutants were accompanied). Two analytical approaches were compared: analysis of all baseline data (all data); versus analysis restricted to baseline data from animals phenotyped on the same day(s) as mutants (accompanying data only). Calculations were based on attaining 80% power while controlling the FDR at 5%. Baseline data comprised 100 days, each with two litters. The variance components used in the power calculations for any particular procedure are shown at the top of the corresponding plot. The vertical axis is restricted to the range [0, 4] so not all curves appear on all panels.

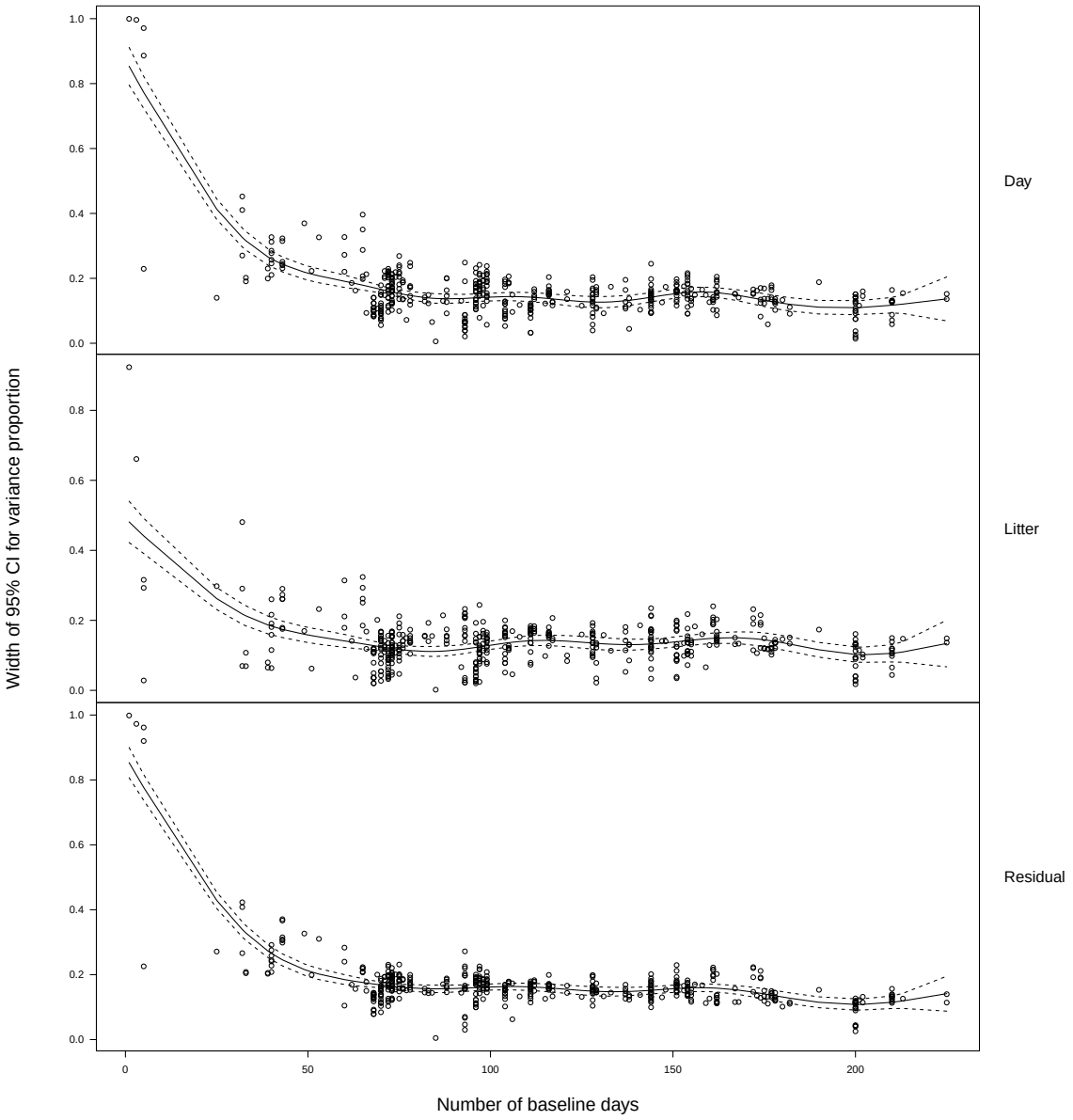

Supplementary Figure 3: Precision of variance component estimates. The precision of variance-component estimates (i.e. width of 95% posterior credible interval) is plotted against the number of baseline days upon which estimation is based. Each point corresponds to a dataset for a particular centre-parameter combination. Smoothing splines were fitted to the data and are superimposed.

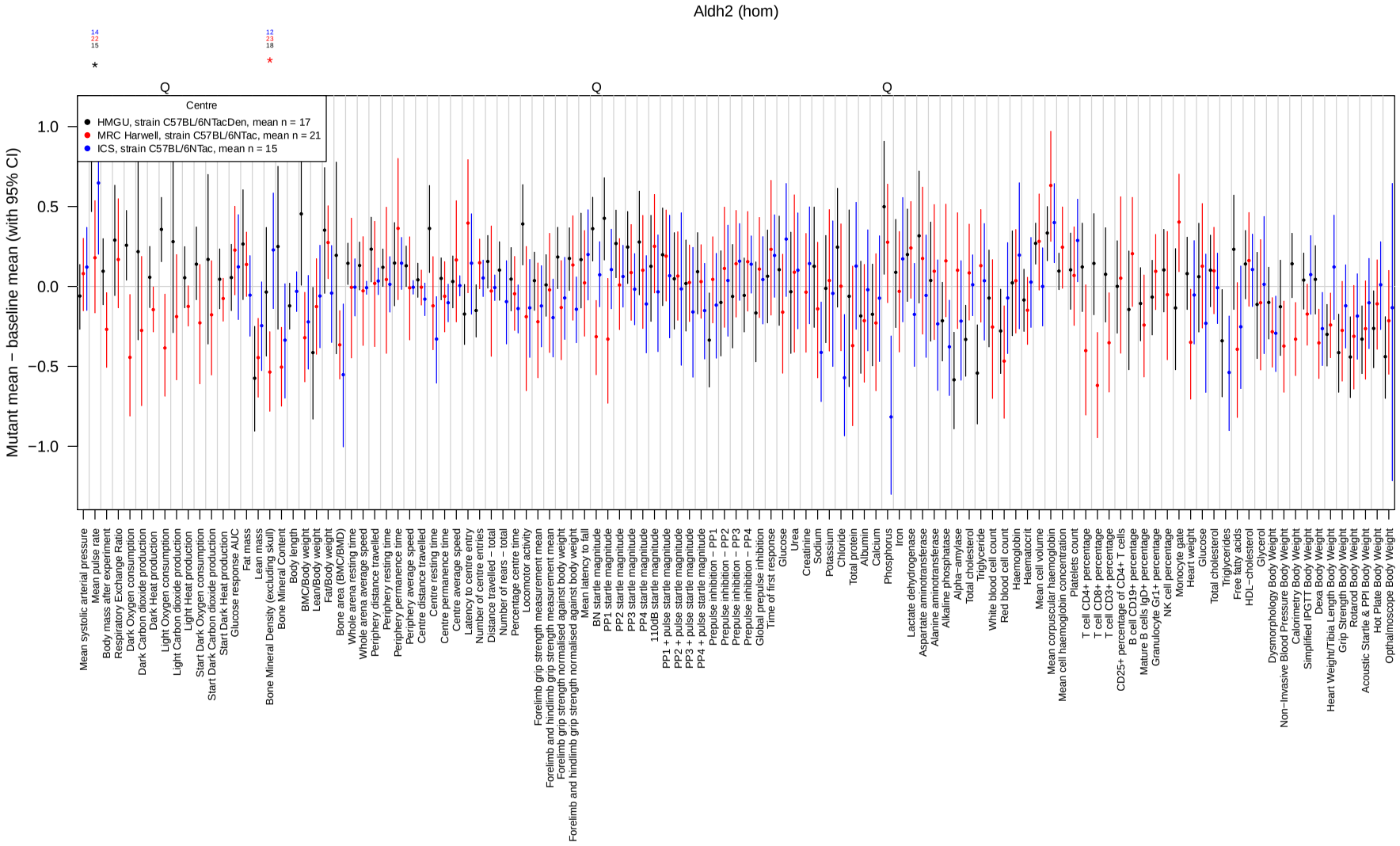

Supplementary Figure 4, Page 1: Comparison of reference lines across centres For each line (one line plotted per page), centre-specific genotype effect estimates and 95% credible intervals are shown. A “Q” indicates significant heterogeneity across centres (see main text for details). A “*” indicates a significant phenotype in the correspondingly coloured centre. Above each significant phenotype, the number of mutant animals phenotyped in each centre is shown in the corresponding colour.

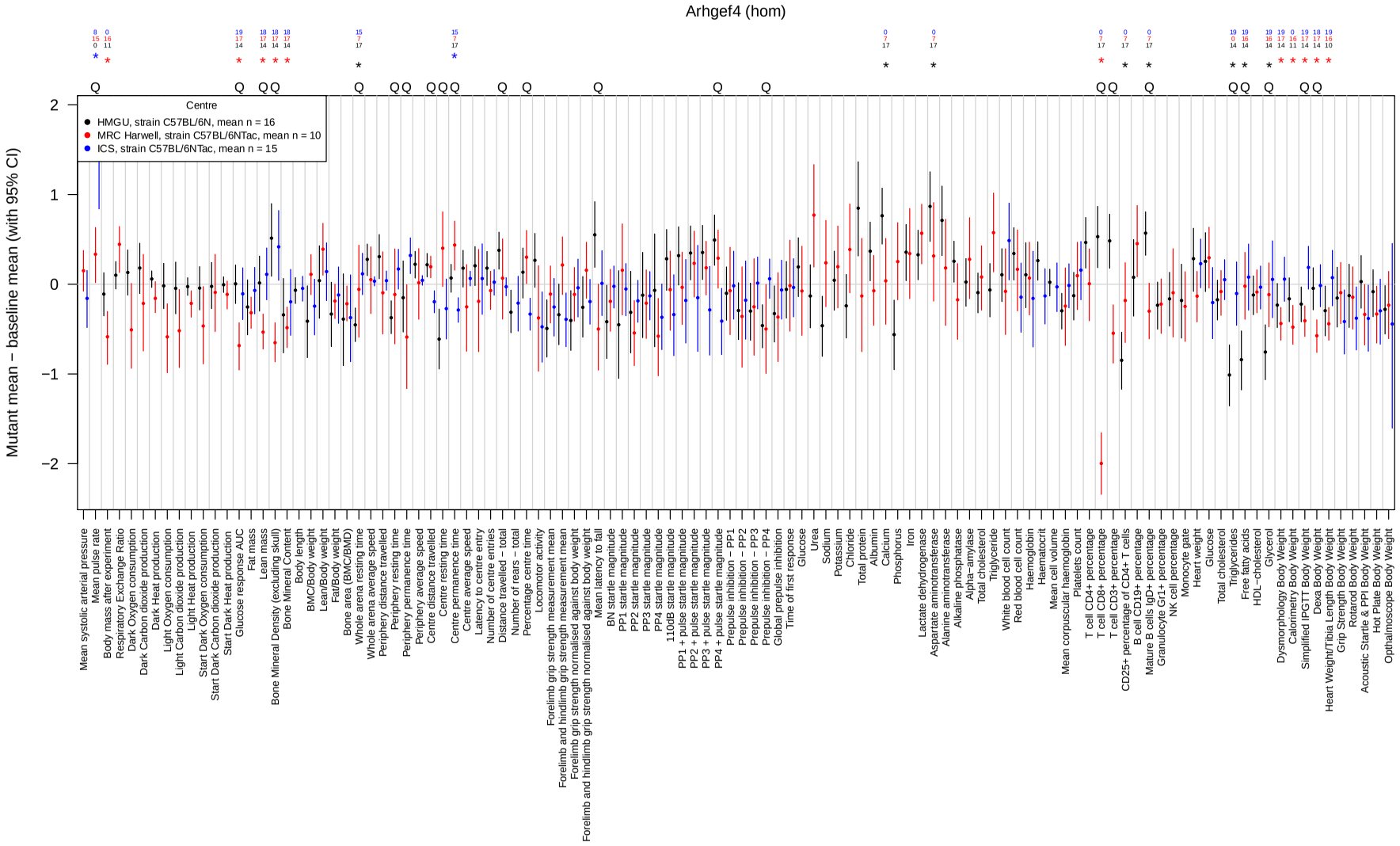

Supplementary Figure 4, Page 2: Comparison of reference lines across centres For each line (one line plotted per page), centre-specific genotype effect estimates and 95% credible intervals are shown. A “Q” indicates significant heterogeneity across centres (see main text for details). A “*” indicates a significant phenotype in the correspondingly coloured centre. Above each significant phenotype, the number of mutant animals phenotyped in each centre is shown in the corresponding colour.

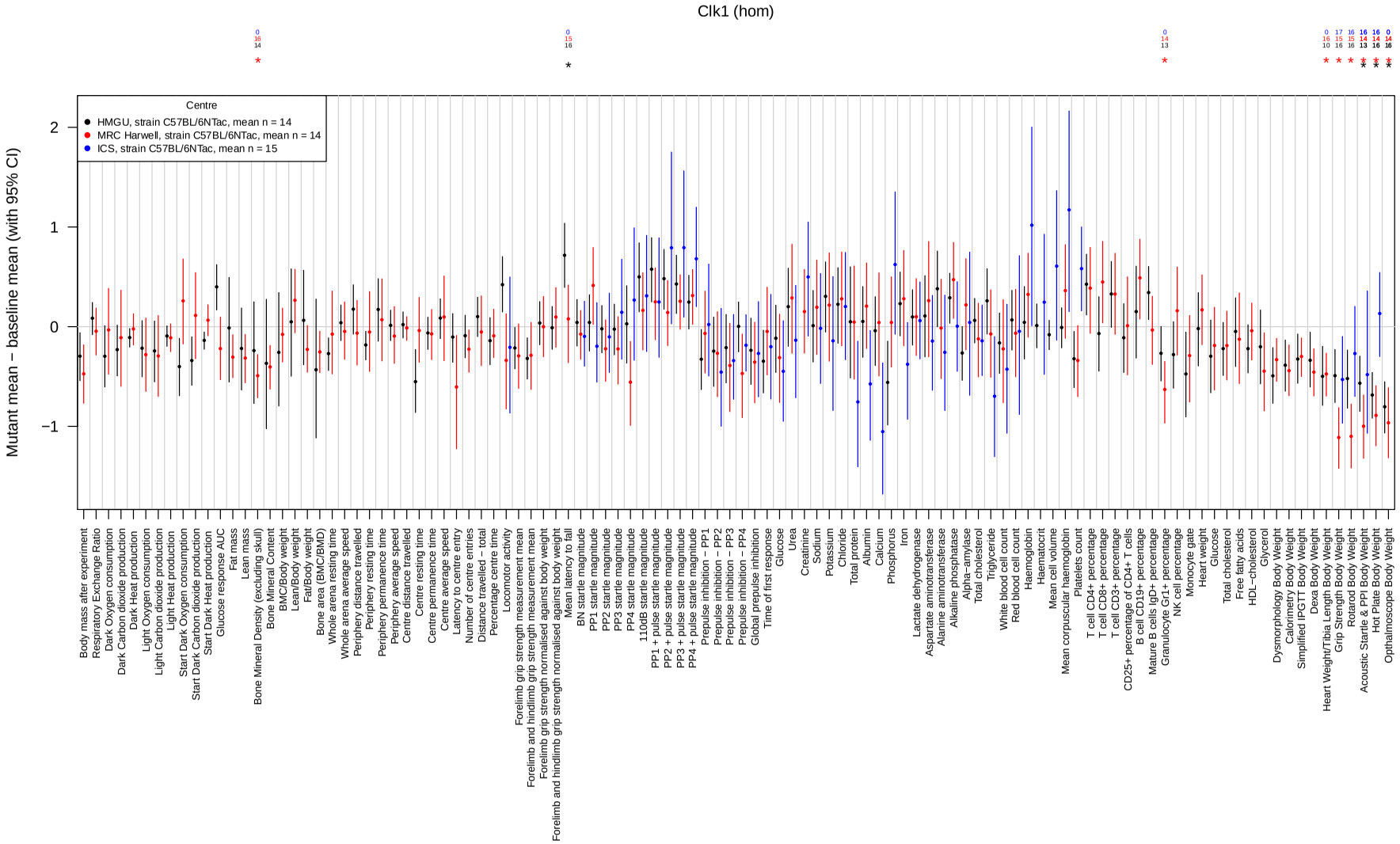

Supplementary Figure 4, Page 3: Comparison of reference lines across centres For each line (one line plotted per page), centre-specific genotype effect estimates and 95% credible intervals are shown. A “Q” indicates significant heterogeneity across centres (see main text for details). A “*” indicates a significant phenotype in the correspondingly coloured centre. Above each significant phenotype, the number of mutant animals phenotyped in each centre is shown in the corresponding colour.

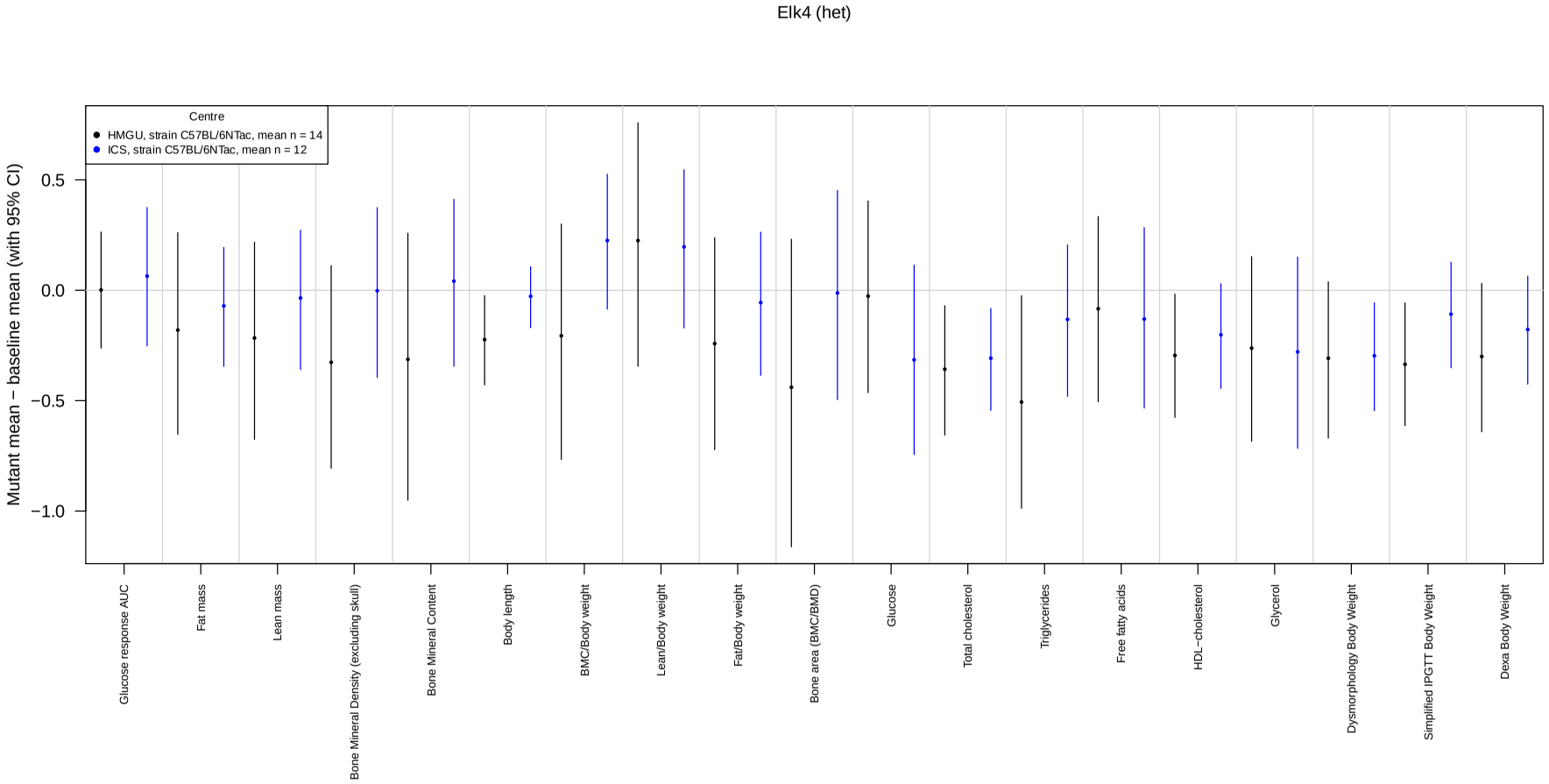

Supplementary Figure 4, Page 4: Comparison of reference lines across centres For each line (one line plotted per page), centre-specific genotype effect estimates and 95% credible intervals are shown. A “Q” indicates significant heterogeneity across centres (see main text for details). A “*” indicates a significant phenotype in the correspondingly coloured centre. Above each significant phenotype, the number of mutant animals phenotyped in each centre is shown in the corresponding colour.

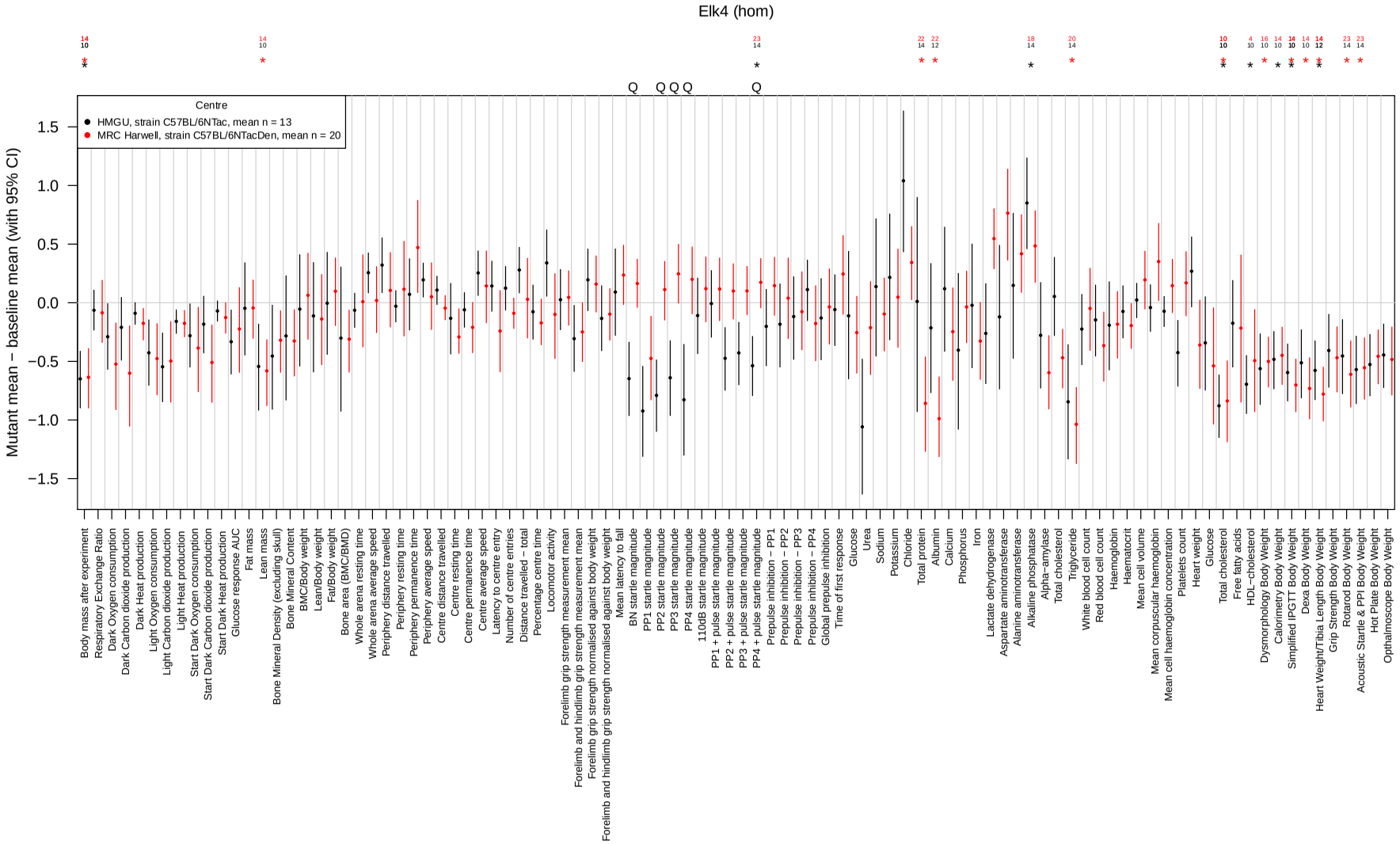

Supplementary Figure 4, Page 5: Comparison of reference lines across centres For each line (one line plotted per page), centre-specific genotype effect estimates and 95% credible intervals are shown. A “Q” indicates significant heterogeneity across centres (see main text for details). A “*” indicates a significant phenotype in the correspondingly coloured centre. Above each significant phenotype, the number of mutant animals phenotyped in each centre is shown in the corresponding colour.

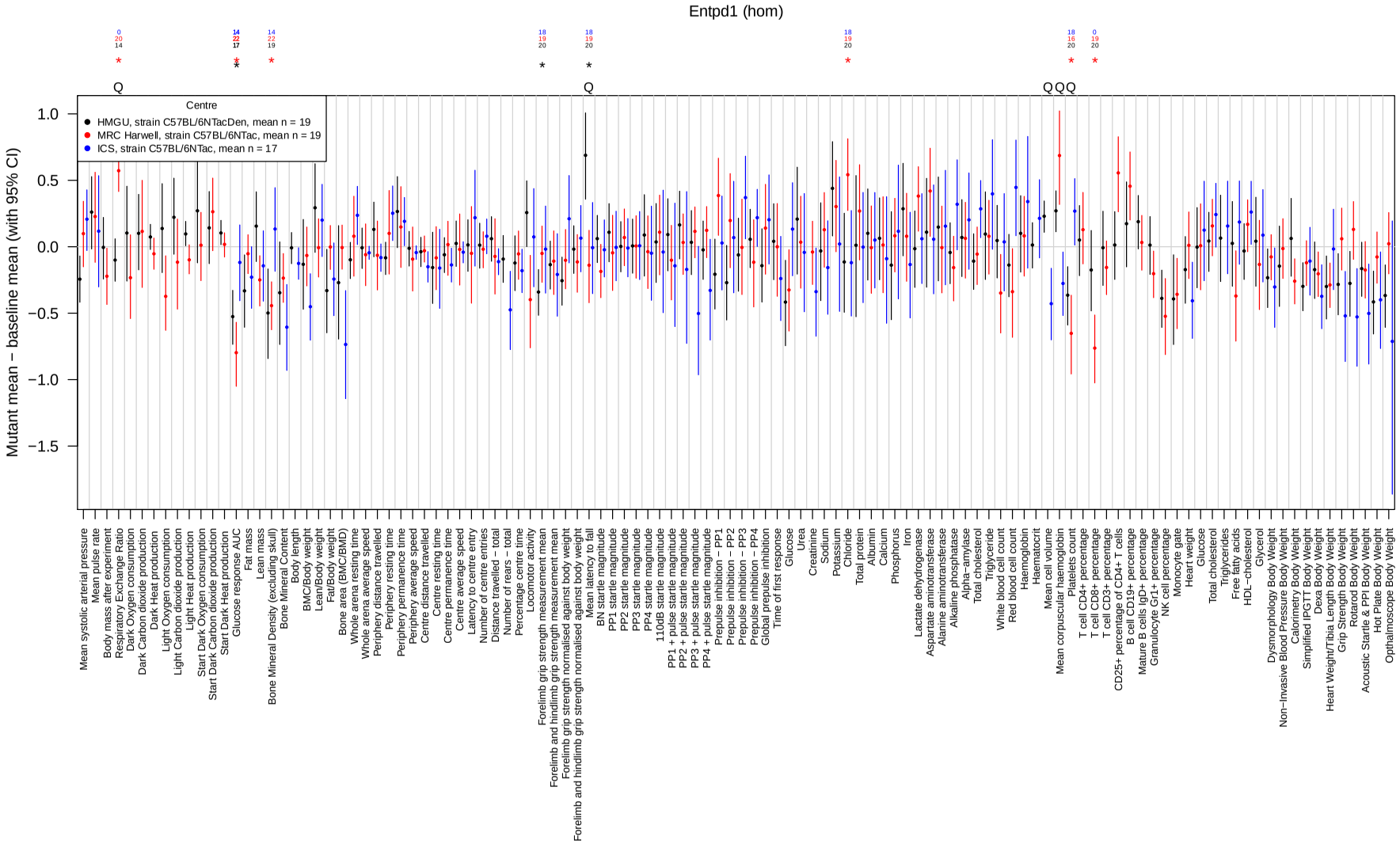

Supplementary Figure 4, Page 6: Comparison of reference lines across centres For each line (one line plotted per page), centre-specific genotype effect estimates and 95% credible intervals are shown. A “Q” indicates significant heterogeneity across centres (see main text for details). A “*” indicates a significant phenotype in the correspondingly coloured centre. Above each significant phenotype, the number of mutant animals phenotyped in each centre is shown in the corresponding colour.

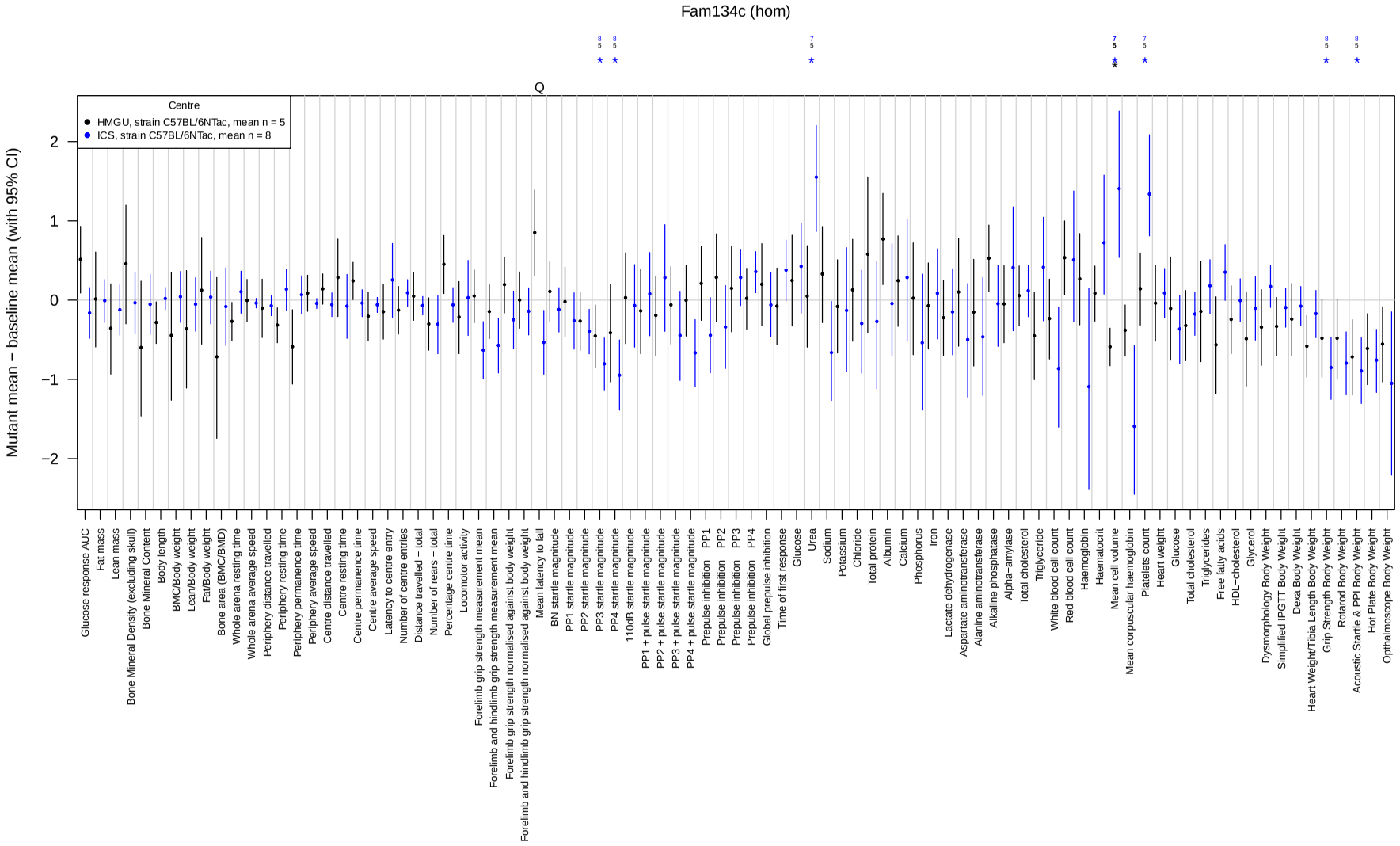

Supplementary Figure 4, Page 7: Comparison of reference lines across centres For each line (one line plotted per page), centre-specific genotype effect estimates and 95% credible intervals are shown. A “Q” indicates significant heterogeneity across centres (see main text for details). A “*” indicates a significant phenotype in the correspondingly coloured centre. Above each significant phenotype, the number of mutant animals phenotyped in each centre is shown in the corresponding colour.

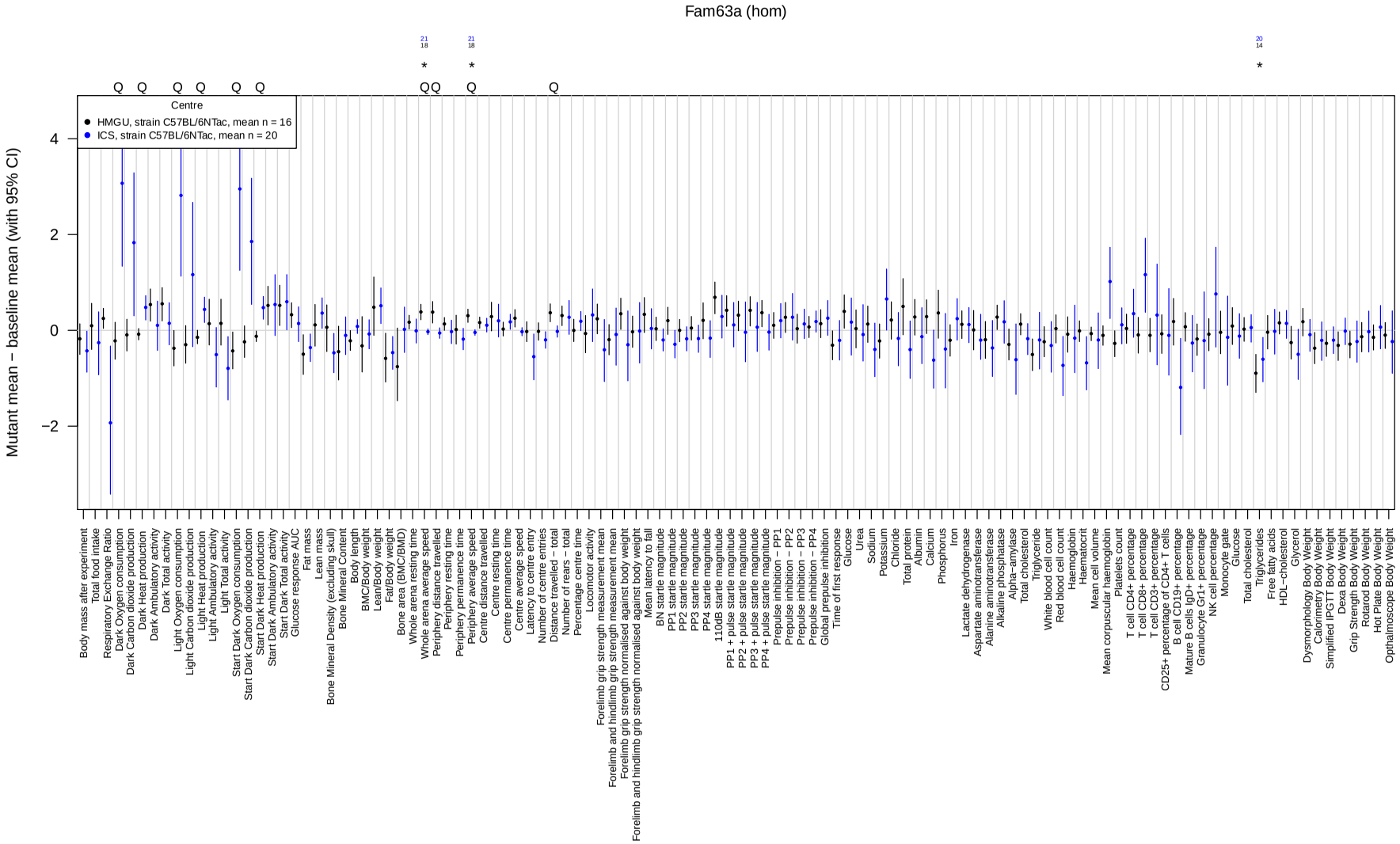

Supplementary Figure 4, Page 8: Comparison of reference lines across centres For each line (one line plotted per page), centre-specific genotype effect estimates and 95% credible intervals are shown. A “Q” indicates significant heterogeneity across centres (see main text for details). A “*” indicates a significant phenotype in the correspondingly coloured centre. Above each significant phenotype, the number of mutant animals phenotyped in each centre is shown in the corresponding colour.

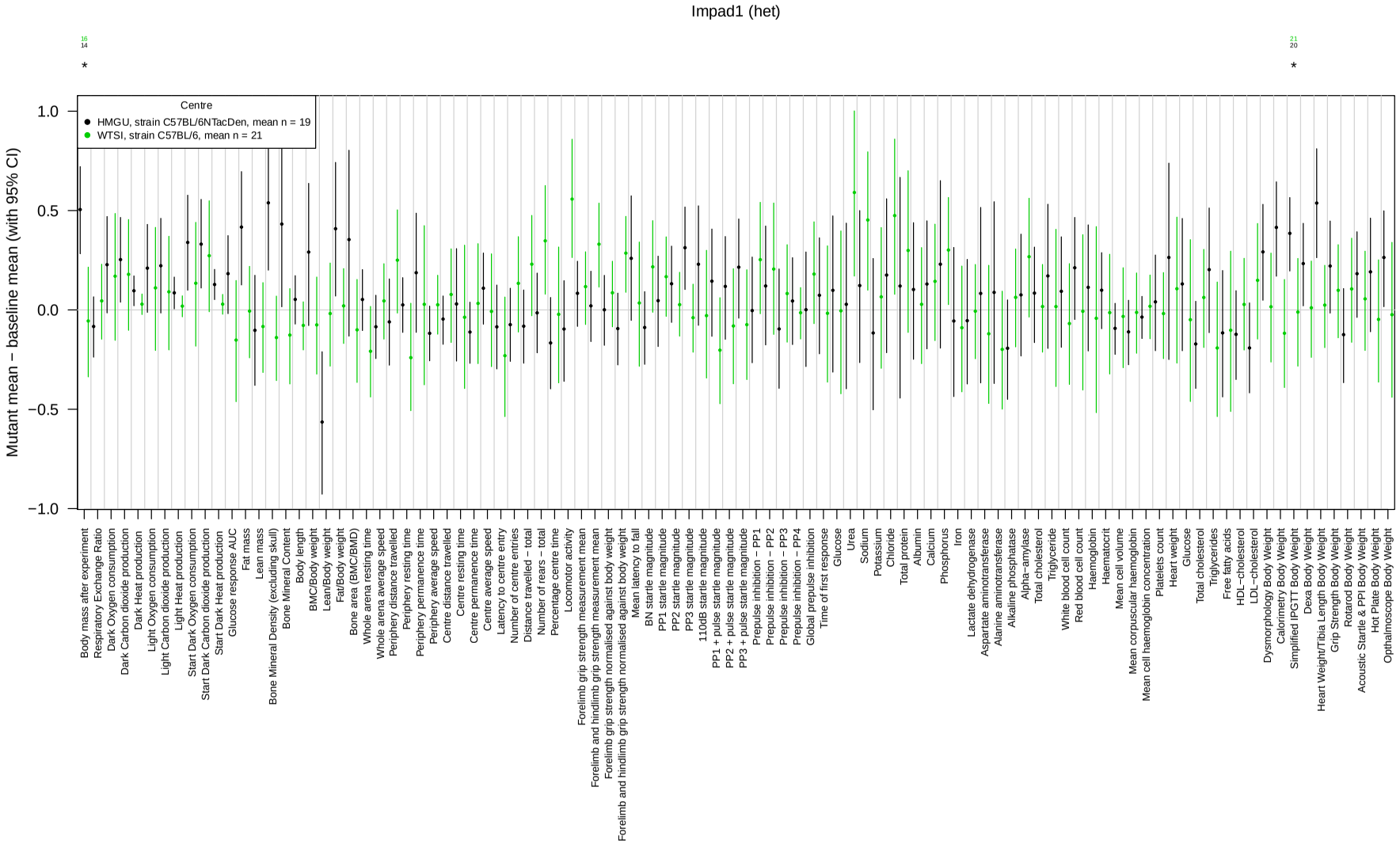

Supplementary Figure 4, Page 9: Comparison of reference lines across centres For each line (one line plotted per page), centre-specific genotype effect estimates and 95% credible intervals are shown. A “Q” indicates significant heterogeneity across centres (see main text for details). A “*” indicates a significant phenotype in the correspondingly coloured centre. Above each significant phenotype, the number of mutant animals phenotyped in each centre is shown in the corresponding colour.

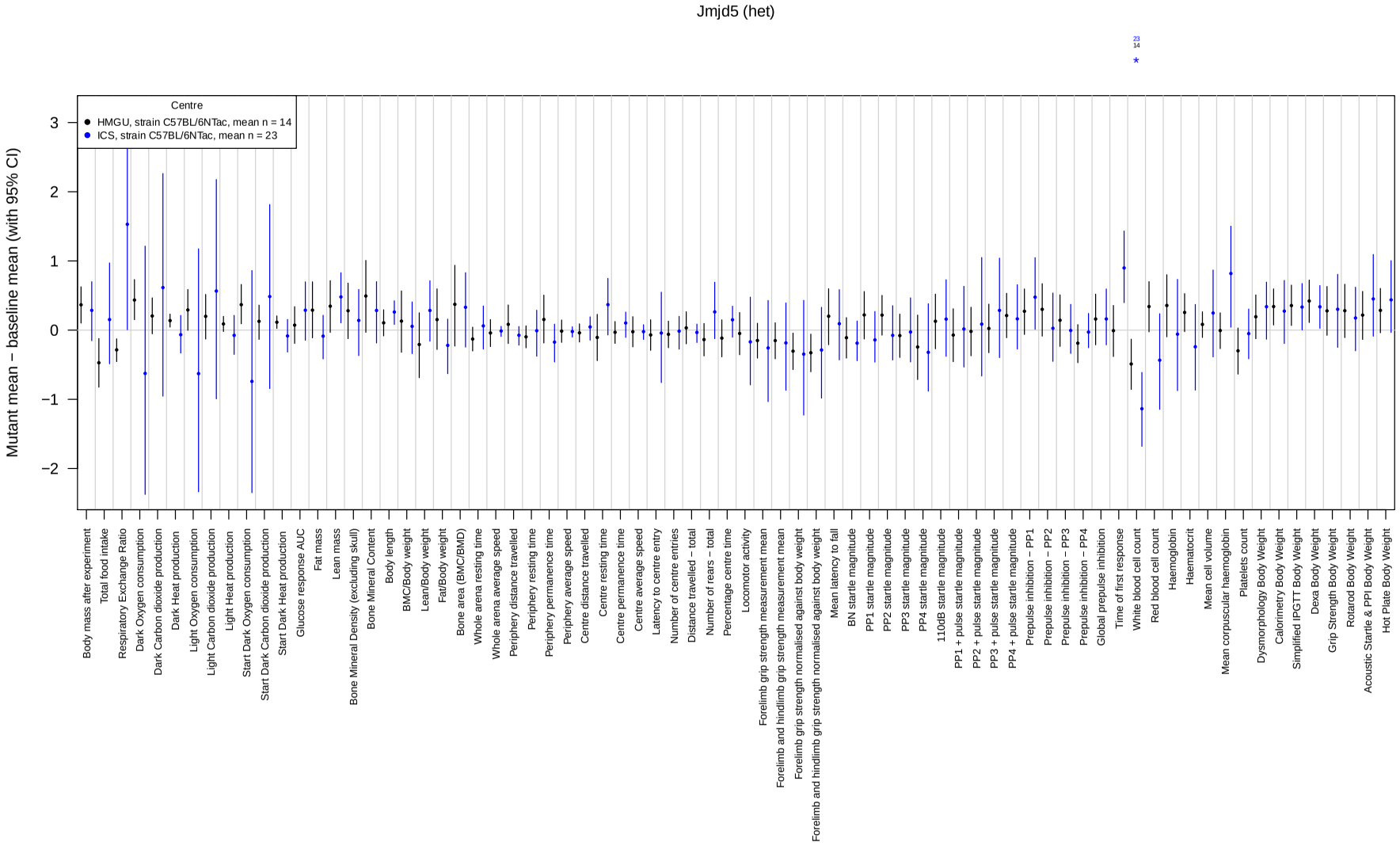

Supplementary Figure 4, Page 10: Comparison of reference lines across centres For each line (one line plotted per page), centre-specific genotype effect estimates and 95% credible intervals are shown. A “Q” indicates significant heterogeneity across centres (see main text for details). A “*” indicates a significant phenotype in the correspondingly coloured centre. Above each significant phenotype, the number of mutant animals phenotyped in each centre is shown in the corresponding colour.

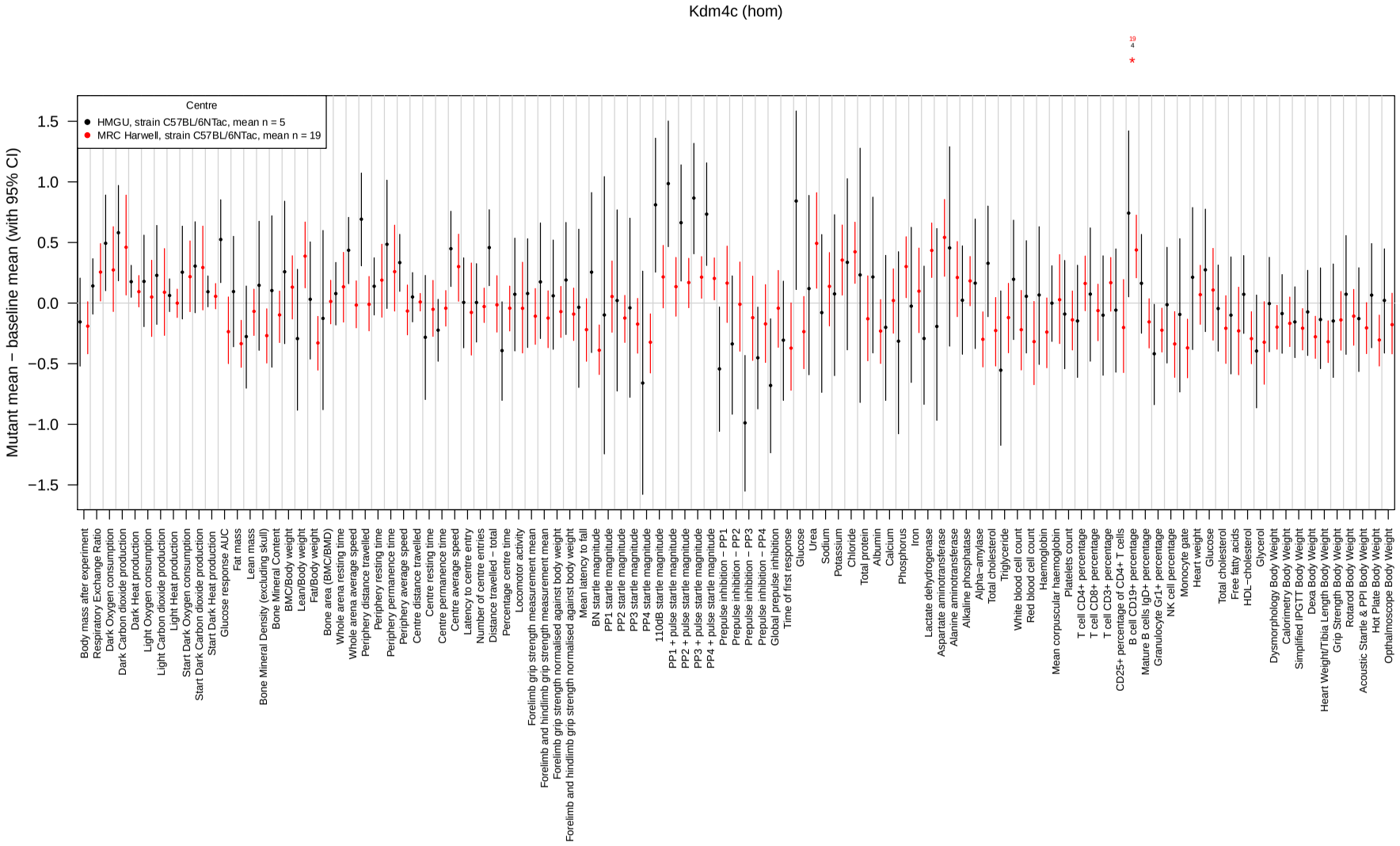

Supplementary Figure 4, Page 11: Comparison of reference lines across centres For each line (one line plotted per page), centre-specific genotype effect estimates and 95% credible intervals are shown. A “Q” indicates significant heterogeneity across centres (see main text for details). A “*” indicates a significant phenotype in the correspondingly coloured centre. Above each significant phenotype, the number of mutant animals phenotyped in each centre is shown in the corresponding colour.

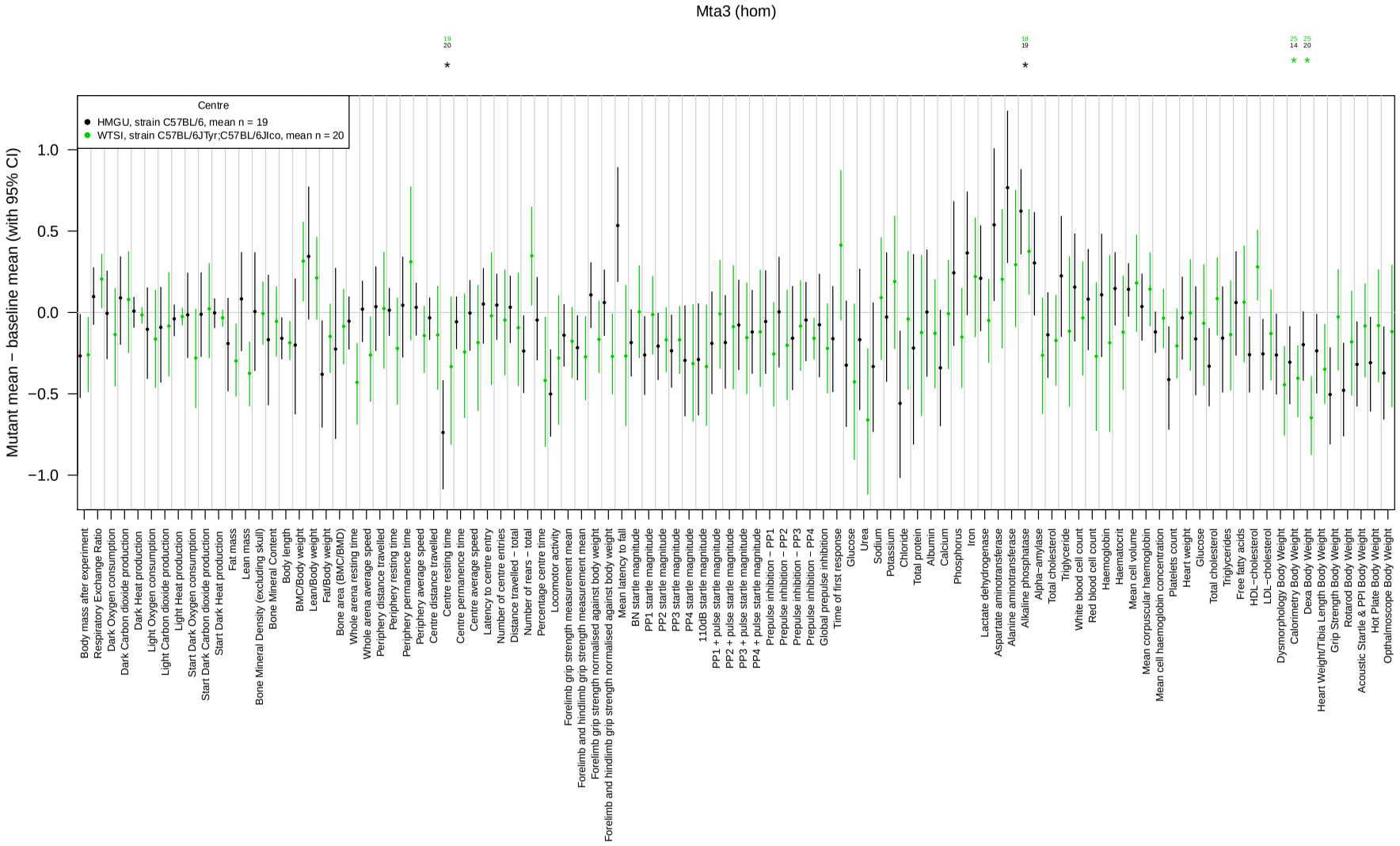

Supplementary Figure 4, Page 12: Comparison of reference lines across centres For each line (one line plotted per page), centre-specific genotype effect estimates and 95% credible intervals are shown. A “Q” indicates significant heterogeneity across centres (see main text for details). A “*” indicates a significant phenotype in the correspondingly coloured centre. Above each significant phenotype, the number of mutant animals phenotyped in each centre is shown in the corresponding colour.

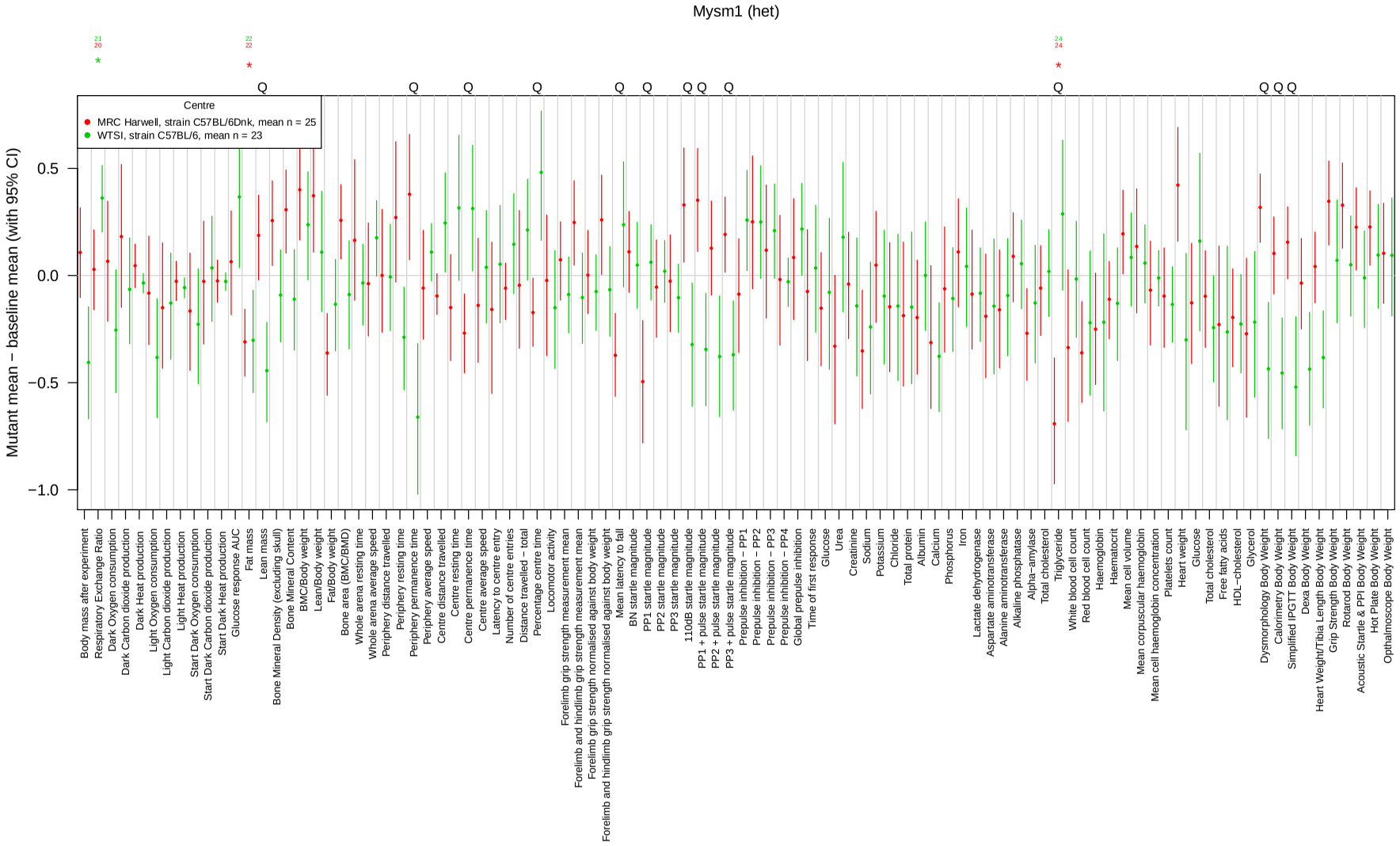

Supplementary Figure 4, Page 13: Comparison of reference lines across centres For each line (one line plotted per page), centre-specific genotype effect estimates and 95% credible intervals are shown. A “Q” indicates significant heterogeneity across centres (see main text for details). A “*” indicates a significant phenotype in the correspondingly coloured centre. Above each significant phenotype, the number of mutant animals phenotyped in each centre is shown in the corresponding colour.

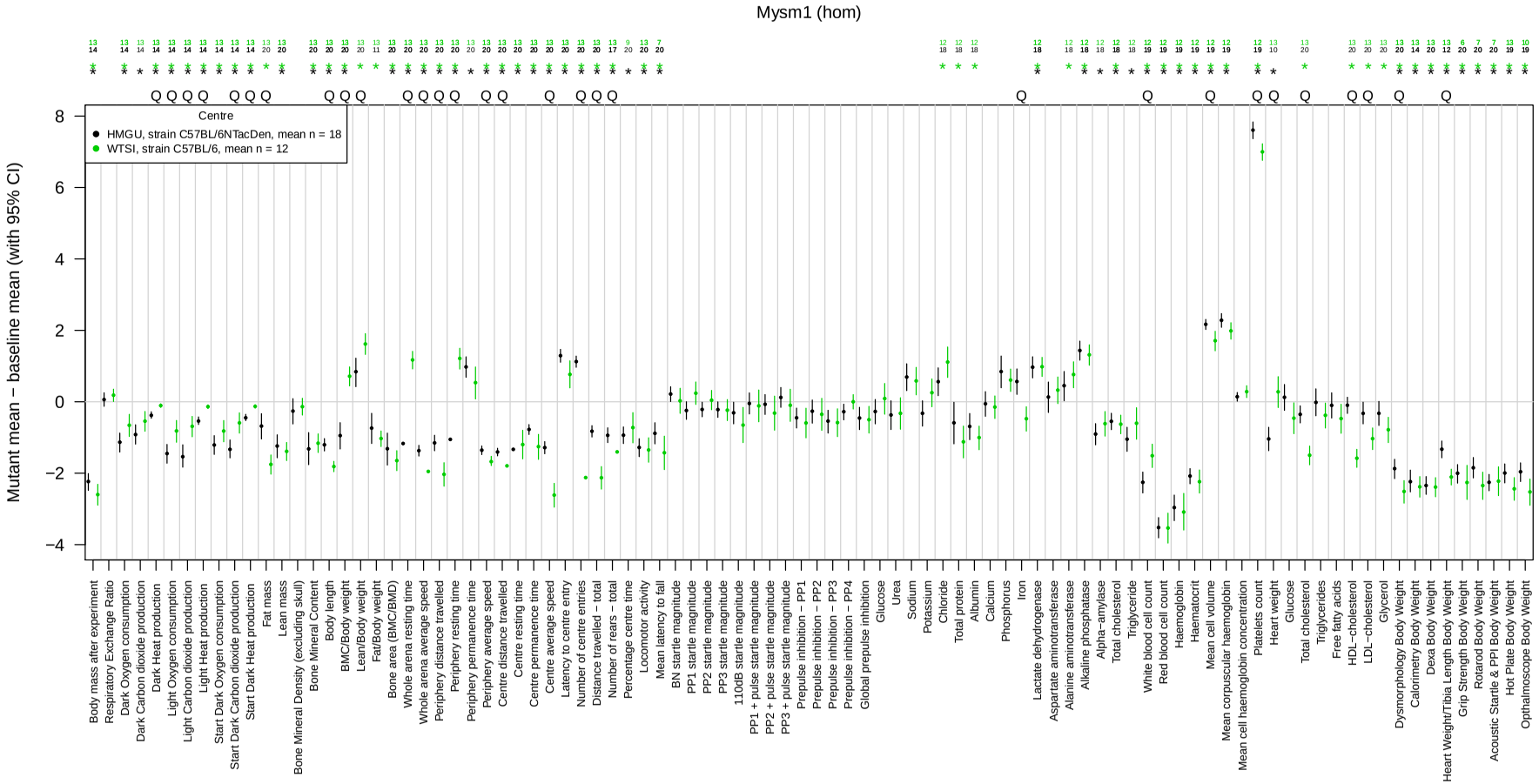

Supplementary Figure 4, Page 14: Comparison of reference lines across centres For each line (one line plotted per page), centre-specific genotype effect estimates and 95% credible intervals are shown. A “Q” indicates significant heterogeneity across centres (see main text for details). A “*” indicates a significant phenotype in the correspondingly coloured centre. Above each significant phenotype, the number of mutant animals phenotyped in each centre is shown in the corresponding colour.

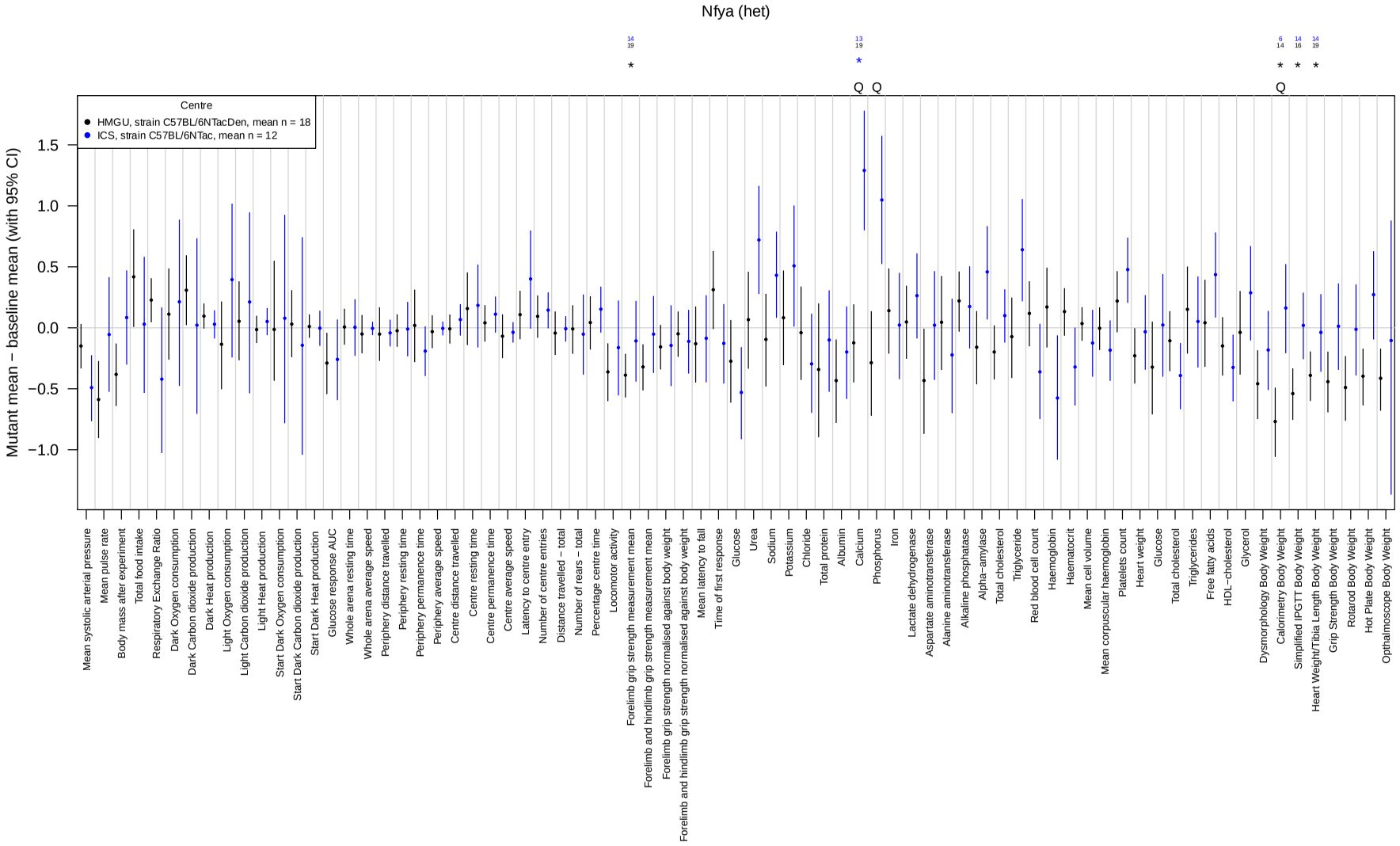

Supplementary Figure 4, Page 15: Comparison of reference lines across centres For each line (one line plotted per page), centre-specific genotype effect estimates and 95% credible intervals are shown. A “Q” indicates significant heterogeneity across centres (see main text for details). A “*” indicates a significant phenotype in the correspondingly coloured centre. Above each significant phenotype, the number of mutant animals phenotyped in each centre is shown in the corresponding colour.

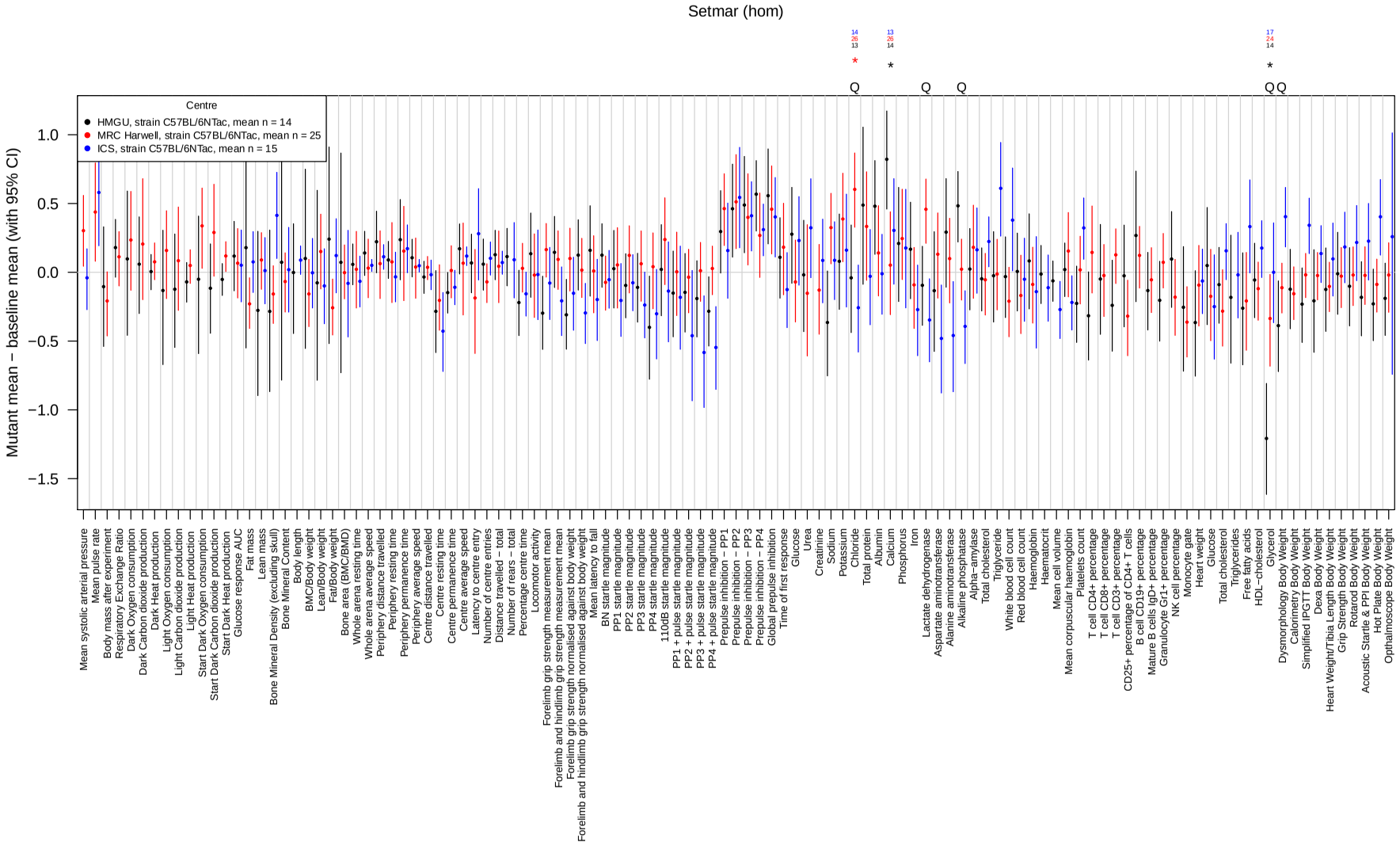

Supplementary Figure 4, Page 16: Comparison of reference lines across centres For each line (one line plotted per page), centre-specific genotype effect estimates and 95% credible intervals are shown. A “Q” indicates significant heterogeneity across centres (see main text for details). A “*” indicates a significant phenotype in the correspondingly coloured centre. Above each significant phenotype, the number of mutant animals phenotyped in each centre is shown in the corresponding colour.

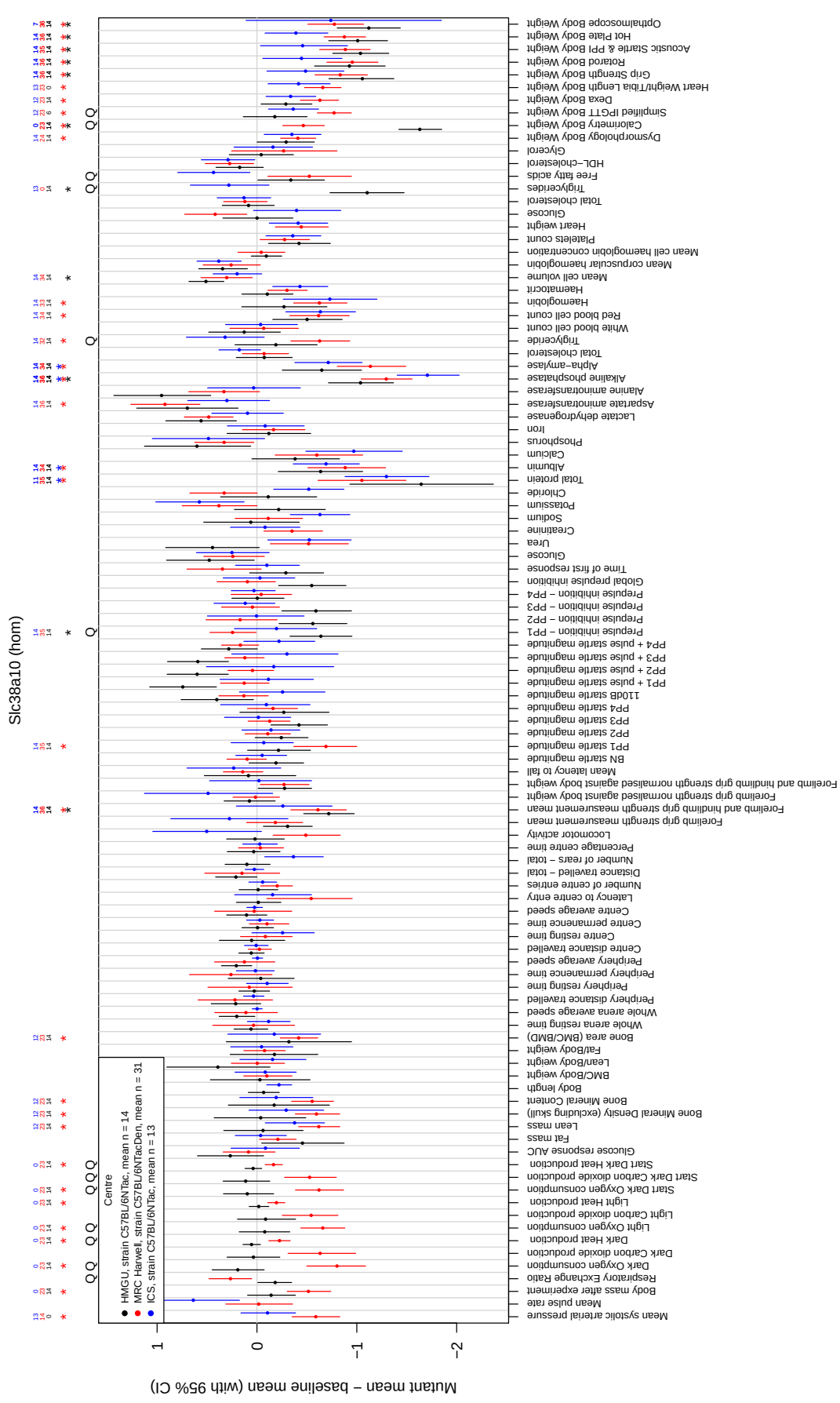

Supplementary Figure 4, Page 17: Comparison of reference lines across centres For each line (one line plotted per page), centre-specific genotype effect estimates and 95% credible intervals are shown. A "Q" indicates significant heterogeneity across centres (see main text for details). A "*" indicates a significant phenotype in the correspondingly coloured centre. Above each significant phenotype, the number of mutant animals phenotyped in each centre is shown in the corresponding colour.

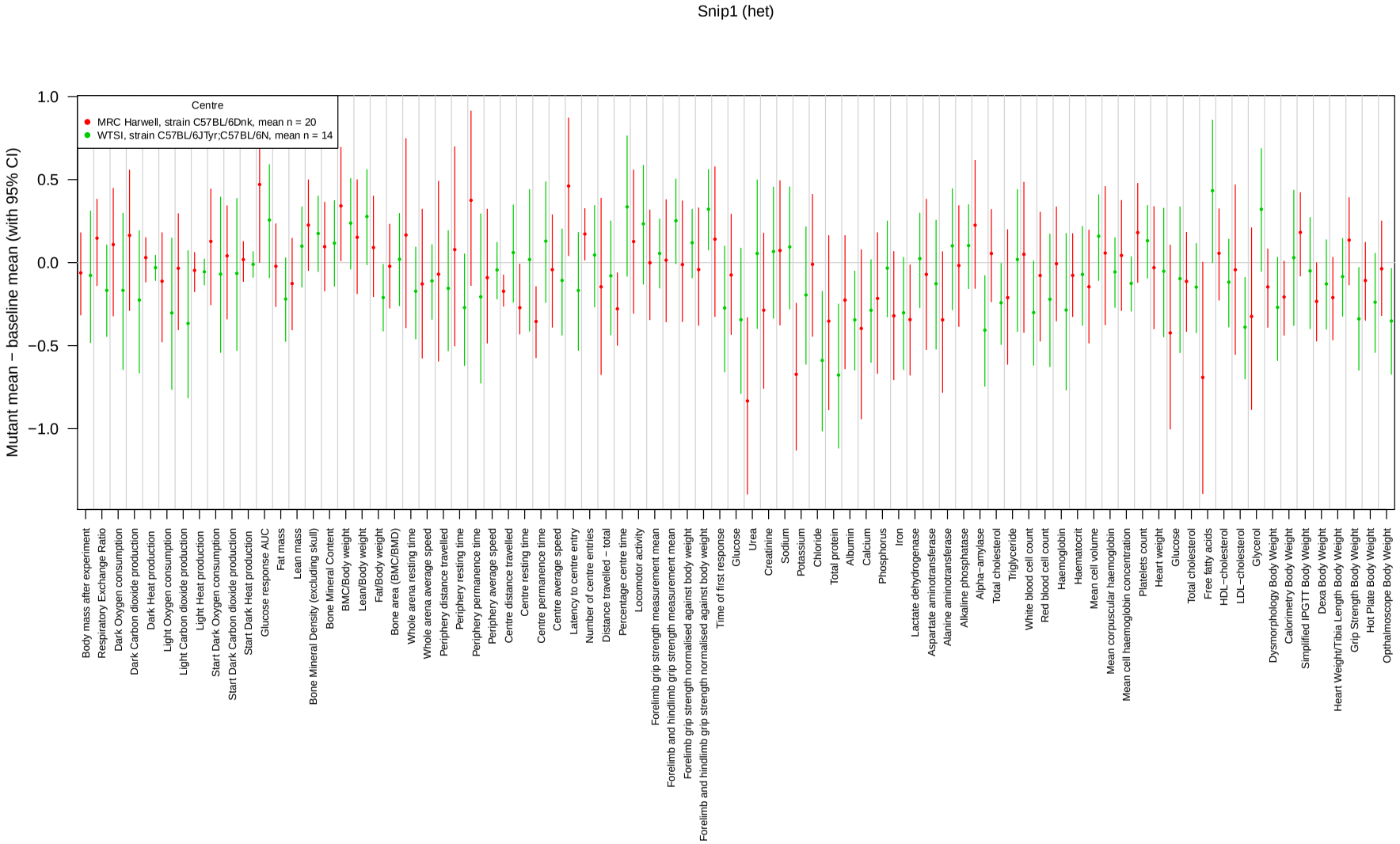

Supplementary Figure 4, Page 18: Comparison of reference lines across centres For each line (one line plotted per page), centre-specific genotype effect estimates and 95% credible intervals are shown. A “Q” indicates significant heterogeneity across centres (see main text for details). A “*” indicates a significant phenotype in the correspondingly coloured centre. Above each significant phenotype, the number of mutant animals phenotyped in each centre is shown in the corresponding colour.

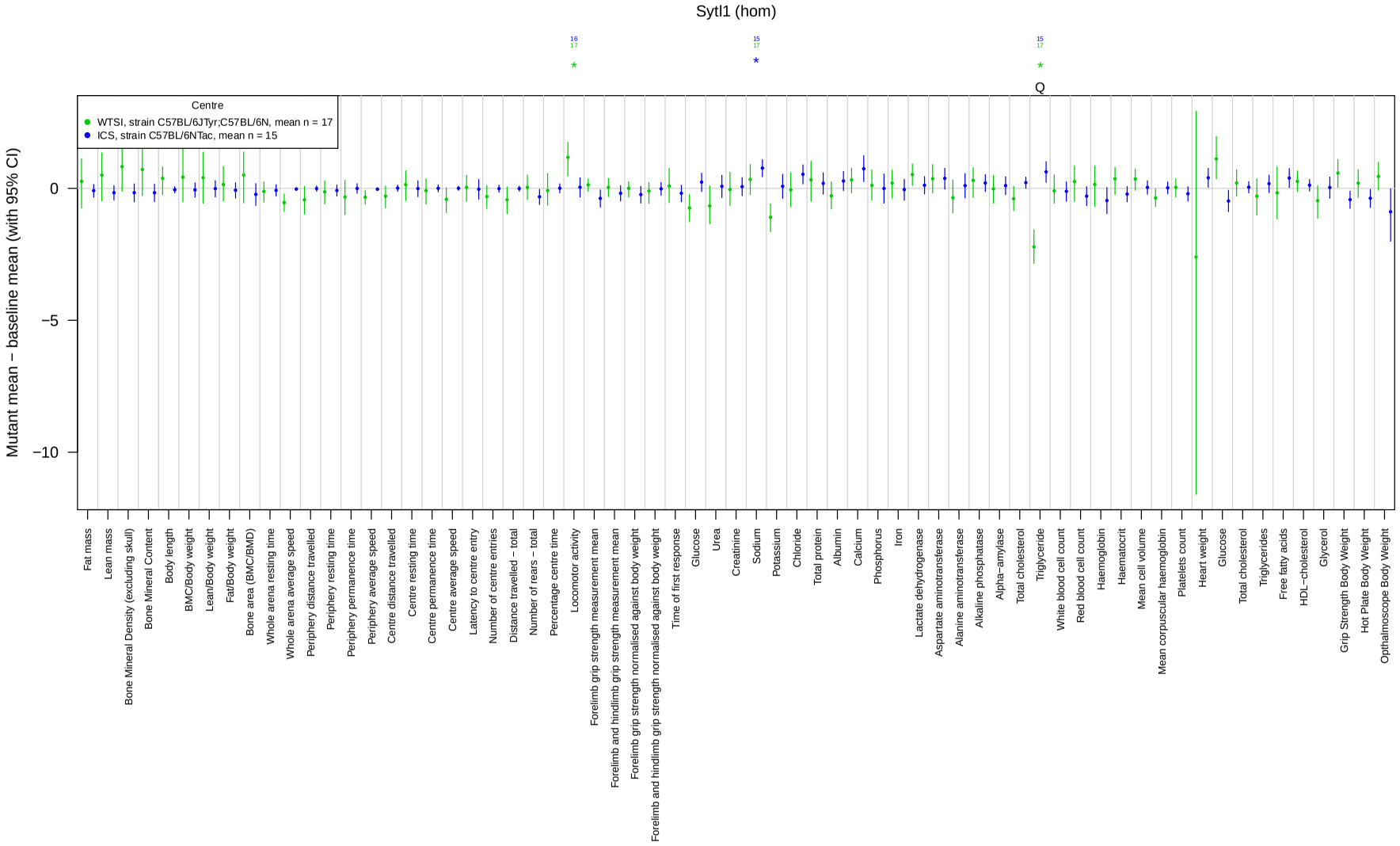

Supplementary Figure 4, Page 19: Comparison of reference lines across centres For each line (one line plotted per page), centre-specific genotype effect estimates and 95% credible intervals are shown. A “Q” indicates significant heterogeneity across centres (see main text for details). A “*” indicates a significant phenotype in the correspondingly coloured centre. Above each significant phenotype, the number of mutant animals phenotyped in each centre is shown in the corresponding colour.

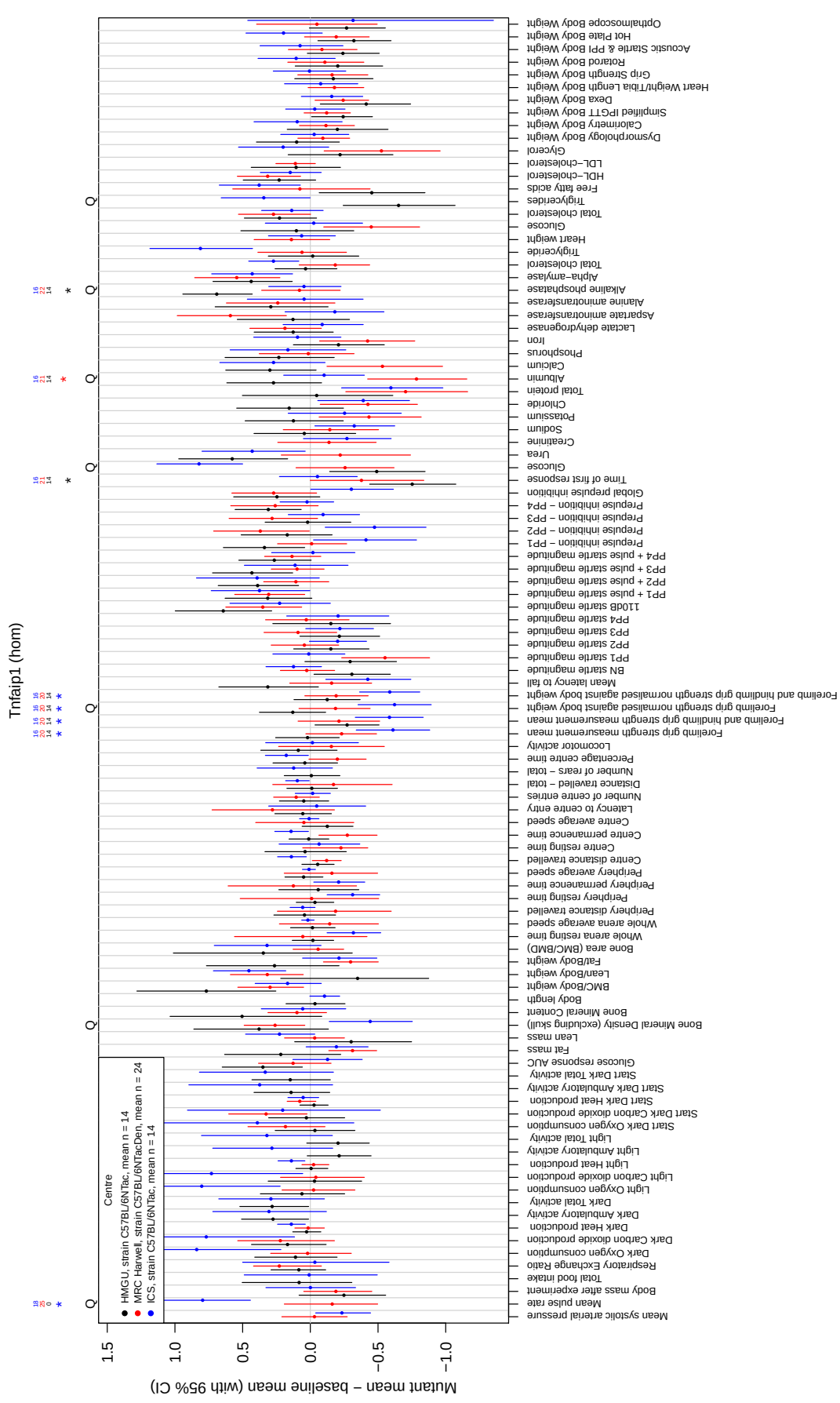

Supplementary Figure 4, Page 20: Comparison of reference lines across centres For each line (one line plotted per page), centre-specific genotype effect estimates and 95% credible intervals are shown. A "Q" indicates significant heterogeneity across centres (see main text for details). A "*" indicates a significant phenotype in the correspondingly coloured centre. Above each significant phenotype, the number of mutant animals phenotyped in each centre is shown in the corresponding colour.

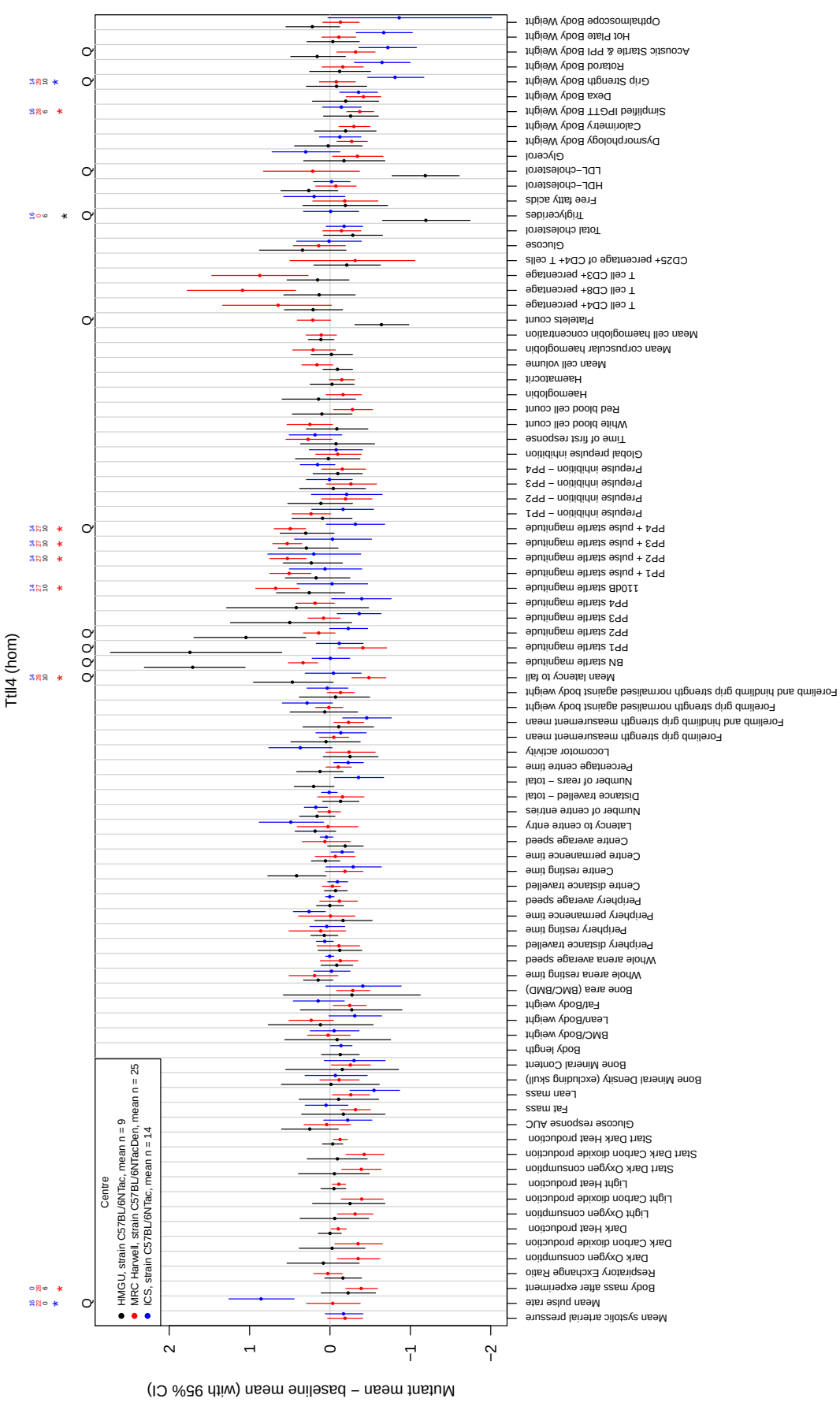

Supplementary Figure 4, Page 21: Comparison of reference lines across centres For each line (one line plotted per page), centre-specific genotype effect estimates and 95% credible intervals are shown. A "Q" indicates significant heterogeneity across centres (see main text for details). A "*" indicates a significant phenotype in the correspondingly coloured centre. Above each significant phenotype, the number of mutant animals phenotyped in each centre is shown in the corresponding colour.

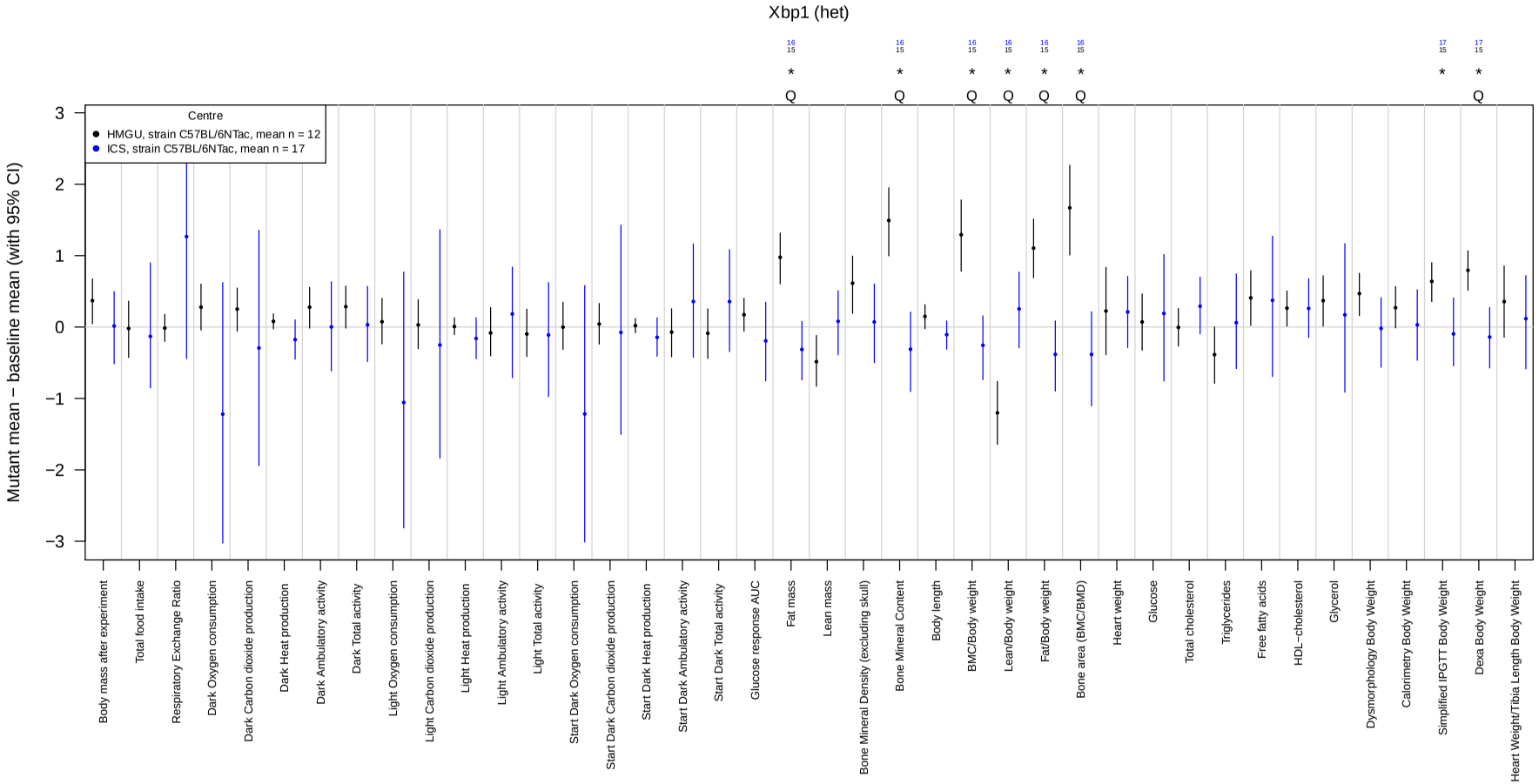

Supplementary Figure 4, Page 22: Comparison of reference lines across centres For each line (one line plotted per page), centre-specific genotype effect estimates and 95% credible intervals are shown. A “Q” indicates significant heterogeneity across centres (see main text for details). A “*” indicates a significant phenotype in the correspondingly coloured centre. Above each significant phenotype, the number of mutant animals phenotyped in each centre is shown in the corresponding colour.

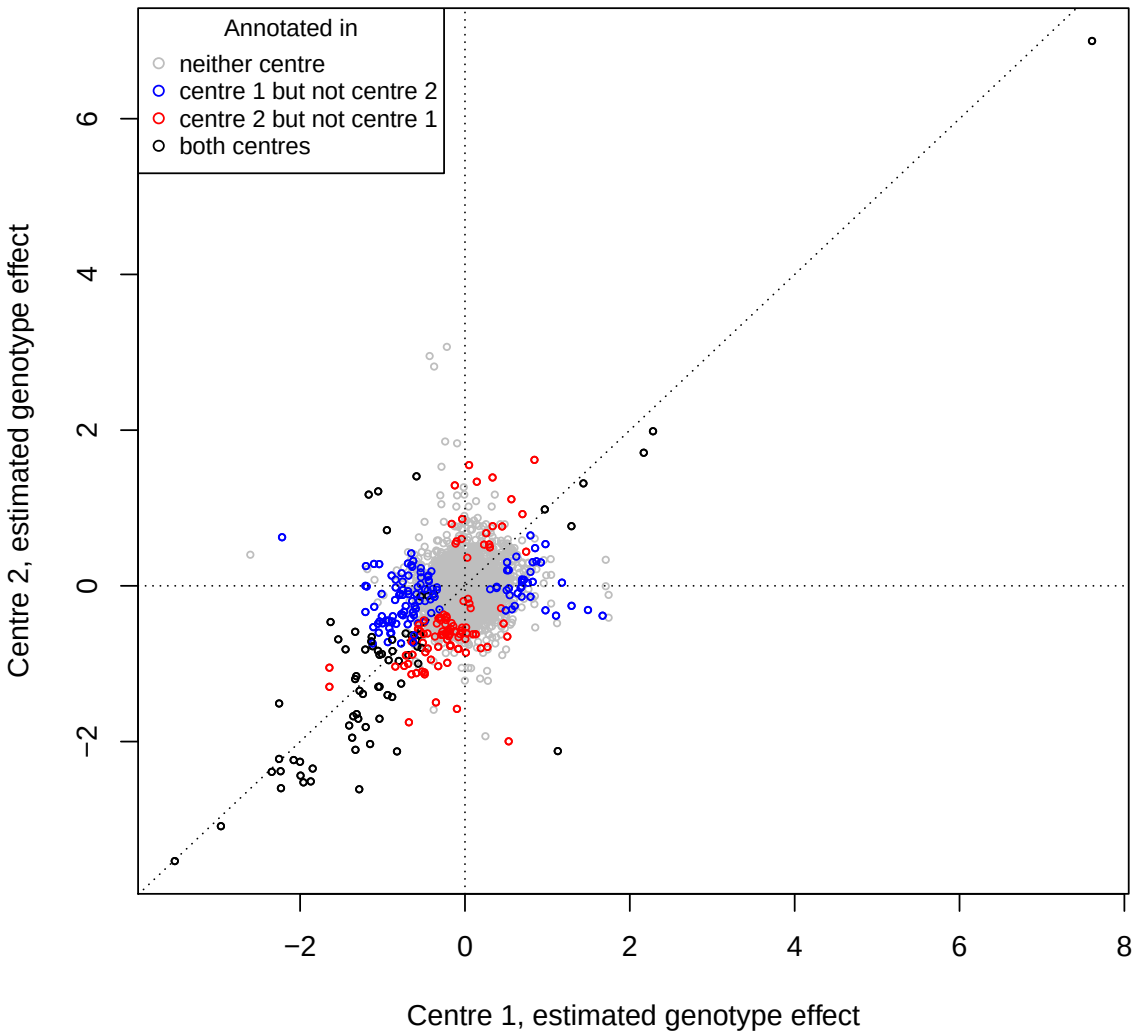

Supplementary Figure 5: Pairwise comparison of reference-line effect estimates across centres. Each point in the plot compares estimated genotype effects across a pair of centres for a reference line phenotyped at both centres. Points are colored according to whether the line was annotated in neither, one, or both of the centres (see legend).

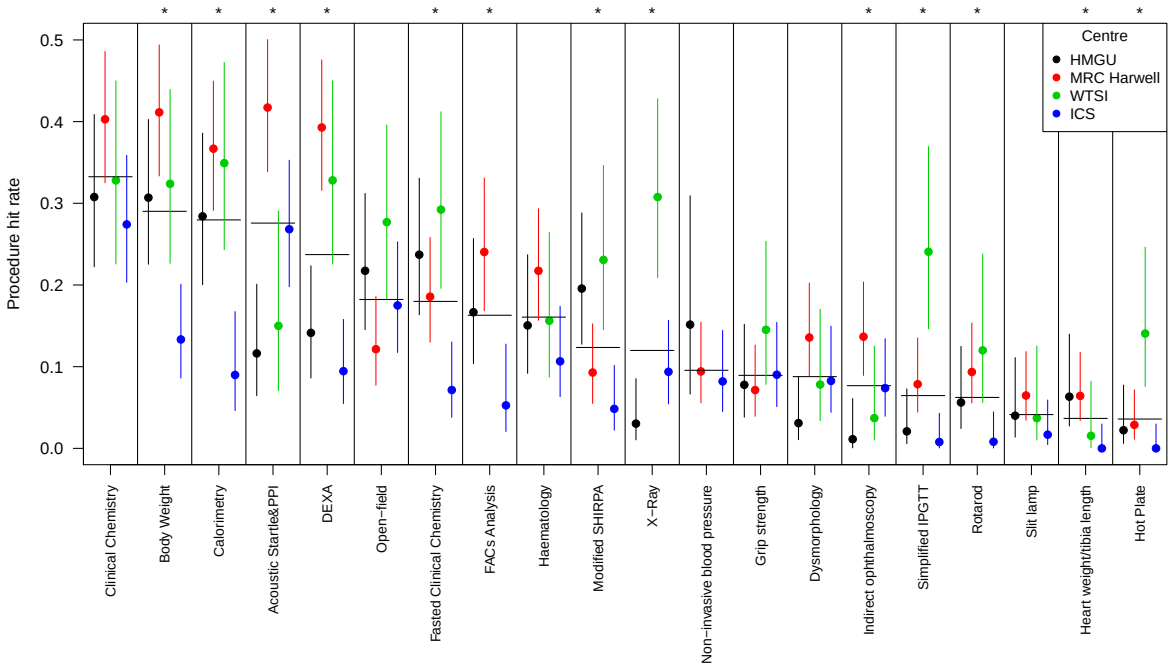

Supplementary Figure 6: Hit rates stratified by procedure and centre. Hit rates stratified by procedure and centre. For each procedure, the proportion of tests (line-parameter combinations) resulting in annotations is indicated by a horizontal black line; centre-specific hit rates are denoted by points, with error bars providing 95% CIs. A "*" denotes procedures with significant inter-centre discordance controlling FDR < 0.05.

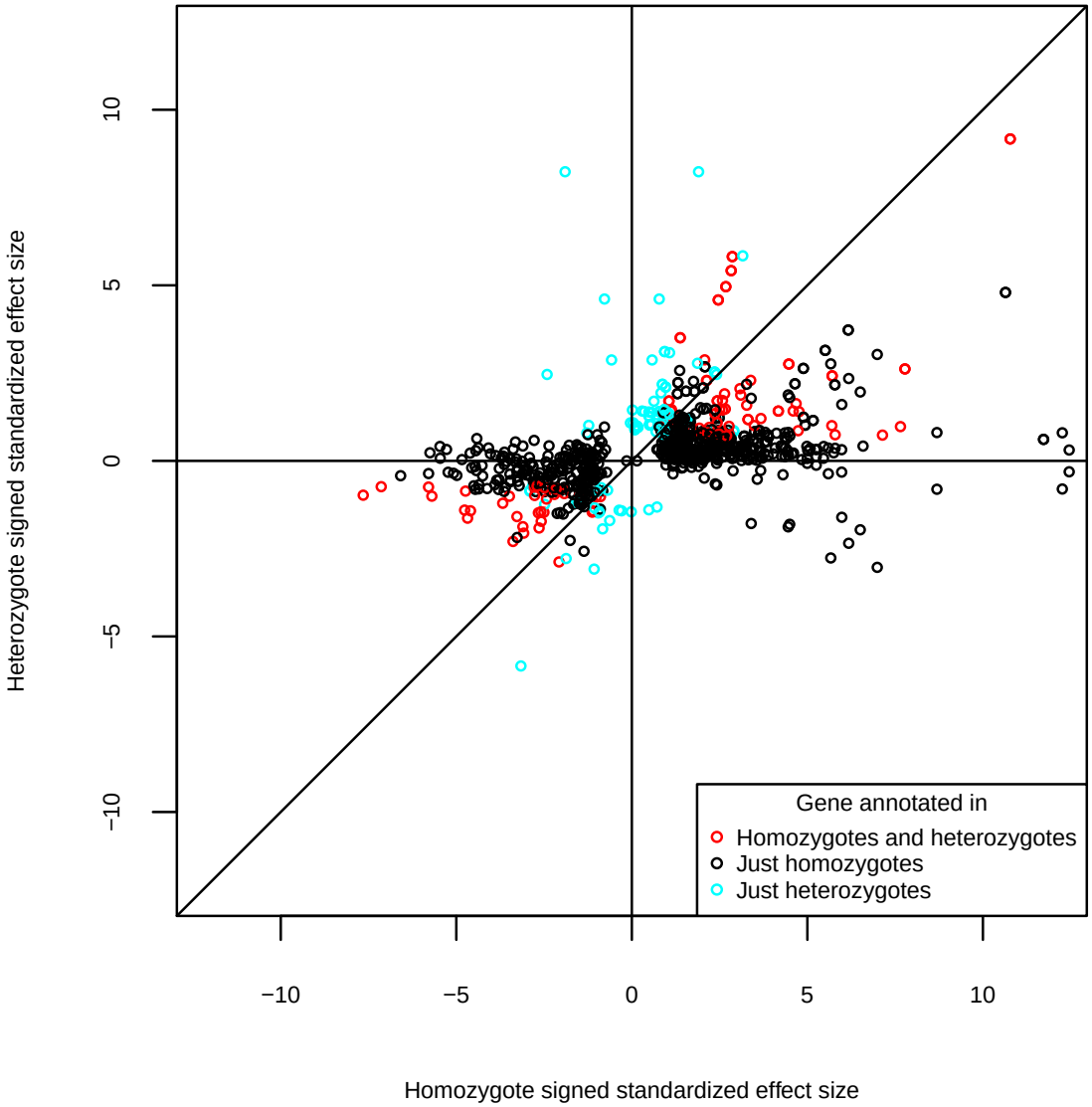

Supplementary Figure 7: Heterozygous versus Homozygous Effect Size Comparison of signed standardized effect size between heterozygotes (vertical axis) and homozygotes (horizontal axis) of the same line. Each point represents a particular combination of a mutant line and a parameter, with the graph only displaying combinations for which at least one of the heterozygote and homozygote is annotated, with zygosity-annotation details being indicated by the point colour (see legend).

II Supplementary Tables

	Lines (number and proportion)			Hit rates		
Centre	Num. Non-EUCOMM	Num. EUCOMM	Prop. Non-EUCOMM	Non-EUCOMM	EUCOMM	All
HMGU	20	81	0.25	0.07	0.04	0.05
MRC Harwell	43	98	0.44	0.12	0.06	0.08
WTSI	24	47	0.51	0.16	0.06	0.09
ICS	28	108	0.26	0.03	0.03	0.03

Supplementary Table 1: Lines and annotation rates at each centre, stratified by non-EUCOMM / EUCOMM.

			HUMAN PHENOTYPES			MOUSE PHENOTYPES	
Gene name	**MGI ID**	**Pubmed Id**	**Databse Annotation***	**Human Description**	**Anatomical system**	**EP Annotation**	**Increased phenotypes****	**Decreased phenotypes****
ABLIM1	MGI:1194500	17486107	**Bipolar Disorder & Obesity**	Bipolar disorder is a condition that affects your moods which can switch from one extreme to another. It includes periods of depression and mania.	Mental Disorder, Body Constitution	Decreased thermal nociceptive threshold	Growth/size,homeostasis/ metabolism,skeleton	Behavior/neurological, integument
ALDH3A2	MGI:1353452	16476818	**Sjögren-Larsson syndrome**	Sjögren-Larsson syndrome is an early childhood-onset disorder with ichthyosis, mental retardation, spastic paraparesis, macular dystrophy, and leukoencephalopathy caused by the deficiency of fatty aldehyde dehydrogenase	Neurological, Eye	Abnormal eye morphology	Integument, vision/eye***	Nervous system, behavior/neurological, homeostasis/metabolism
ELMOD1	MGI:3583900	20585627	**Behavior and Behavior Mechanisms**	Personality traits and preferences including optimism and preference for night-time versus morning-time activity.	Behavior and Behavior Mechanisms	Increased hyperactivity and trunk curl. Abnormal locomotor activation, behaviour and gait Decreased grip strength, body weight, prepulse inhibition. Abnormal behaviour and hyperactivity.	Behavior/neurological,immune system,hematopoietic system,homeostasis/metabolism	Growth/size,nervous system, behavior/neurological, homeostasis/metabolism, hematopoietic system, immune system
FRMD5	MGI:2442557	20686565	**Triglycerides**	Triglycerides are a major form of fat stored by the body. Plasma concentrations of triglycerides alongside other lipids are among the most important risk factors for coronary artery disease.	Metabolic	Increased body weight and abnormal body weight	Growth/size	Nervous system, behavior/neurological
KCTD10	MGI:2141207	19060906	**Lipoproteins, HDL cholesterol**	Levels of liproproteins, triglycerides and total cholesterol are heritable, modifiable risk factors for many disorders including coronary artery disease.	Metabolic	Increased circulating creatine kinase level	Homeostasis/metabolism, limbs/digits/tail, skeleton	Homeostasis/metabolism, skeleton

Supplementary Table 2, Page 1: Concordance of novel genes with human disease data.

MCF2L	MGI:103263	17634449	**Coronary Artery Disease, Stroke**	Coronary Artery Disease is caused by plague build up in the arteries which can block blood flow.	Cardiovascular, Nervous system	Increased monocyte cell number Decreased circulating glycerol level and prepulse inhibition	Immune system,hematopoietic system	Nervous system, homeostasis/metabolism
MRPL10	MGI:1333801	23535033	**Alzheimer's disease (cognitive decline)**	Alzheimer's disease is a devastating neurological disorder primarily affecting the elderly. The disease manifests with progressive deterioration in cognitive functions, leading to loss of autonomy.	Nervous System, Mental Disorders	Decreased abnormal behaviour.	Behavior/neurological	
NDUFAF 6	MGI:1924197	24162737	**Leigh syndrome with leukodystrop hy**	Alzheimer's disease is a neurological disorder primarily affecting the elderly. The disease is characterised by progressive deterioration in cognitive functions, leading to loss of autonomy.	Nervous System	Increased tremors and abnormal gait. Decreased hypoactivity and prepulse inhibition	Growth/size, skeleton, homeostasis/metabolism	Nervous system, behavior/neurological
OPTN	MGI:1918898	21623375	**Paget's disease**	Paget Disease is characterised by focal areas of increased and disorganised bone remodeling that may lead to bone pain, bone deformity, pathological fracture, deafness and secondary osteoarthritis.	Bone Diseases	Abnormal bone mineralization and bone structure.	Digestive/alimentary phenotype***	Skeleton, growth/size, immune system, hematopoietic system
PARVB	MGI:2153063	23535911	**Non-alcoholic fatty liver disease**	A build up of fat within the liver cells. Usually seen in people who are overweight or obese.	Liver Diseases	Increased granulocyte number and monocyte cell number.	Immune system, hematopoietic system	Homeostasis/metabolis m, hematopoietic system
TTC39B	MGI:1917113	24097068	**Lipoproteins, HDL cholesterol**	Levels of liproproteins, triglycerides and total cholesterol are heritable, modifiable risk factors for many disorders including coronary artery disease.	Metabolic	Decreased circulating triglyceride level	Homeostasis/metabolism	Homeostasis/metabolis m, behavior/neurological

Supplementary Table 2, Page 2: Concordance of novel genes with human disease data.

USP12	MGI:1270128	17460697	**Diabetes Mellitus, Type 2**	Type II diabetes mellitus is associated with increased blood concentrations of markers including cytokines, serum amyloids and interleukins.	Metabolic	Decreased mean corpuscular volume, mean corpuscular hemoglobin concentration, CD8-positive, alpha-beta T cell number and T cell number Increased Alpha-amylase level.	Homeostasis/metabolism	Immune system,hematopoietic system phenotype
USP12	MGI:1270128	19915573	**Ulcerative colitis**	Ulcerative colitis is a major phenotype of inflammatory bowel disease (IBD) that is characterized by repeated chronic inflammation of the gastrointestinal tract. Cytokines, antibodies and complement proteins promote inflammation. Inflammation occurs because these molecules attract immune system cells to the affected tissue.	Digestive System Diseases	Decreased mean corpuscular volume, mean corpuscular hemoglobin concentration, CD8-positive, alpha-beta T cell number and T cell number	Homeostasis/metabolism	Immune system,hematopoietic system phenotype
VAT1L	MGI:2142534	23535033	**Alzheimer Disease**	Alzheimer's disease is a neurological disorder primarily affecting the elderly. The disease is characterised by progressive deterioration in cognitive functions, leading to loss of autonomy.	Mental Disorder, Nervous System	Abnormal behaviour.	Behavior/neurological	Behavior/neurological phenotype

*** Databases are Gwas Central, Gwas Catalogue and Orphanet, **Top-level phenotypes, ***Categorical data**

Supplementary Table 2, Page 3: Concordance of novel genes with human disease data.

III Supplementary Note

III.1 Statistical Methods

III.1.1 Analysis of quantitative phenotypes

A transformation was applied to each quantitative phenotype separately, and to data from across all phenotyping centres at once. For any quantitative phenotype with some observations ≤ 0, a constant was added to all observations prior to transformation in order to satisfy: $\min(y) = (\max(y) - \min(y))/100$. Phenotypes were then Box-Cox transformed with the exponent λ constrained to be in $\lambda \in \{-2, -1.5, \ldots, 1.5, 2\}$ and chosen to maximise the likelihood with respect to λ under an ordinary Gaussian linear model applied to data from baseline animals with sex and day as covariates. After Box-Cox transformation, each phenotype's data were scaled to zero mean and unit standard deviation.

Transformed quantitative phenotypes were then analysed under a Gaussian-response Bayesian multilevel model with day (α^{day}), litter (α^{litter}), genotype (β^{geno}), sex (β^{sex}), strain (β^{strain}), investigator (β^{inv}) and metadata group (β^{meta}) as covariates, and with a penalized spline to account for systematic temporal trends in baseline animal measurements. The penalized spline was fitted as described in chapter 16 of [1], with the pure cubic polynomial component having coefficients β^{poly}, and the full cubic spline's basis functions having coefficients α_k^{spl} which were regularised via a hierarchical model with variance component σ^2_{spl}. Day and litter effects were modelled hierarchically with variance components σ^2_{day} and σ^2_{litter}. The residual variance is denoted by σ^2_{resid}. For any particular mutant line the analysis was restricted to data from that line along with data from all baseline animals at the same centre. The model was:

$$
\begin{aligned}
y_i &\sim N\left(\mu_i,\ \sigma^2_{\text{resid}}\right) \\
\mu_i &= \alpha^{\text{day}}_{d[i]} + \alpha^{\text{litter}}_{l[i]} + \sum_{k=1}^{K+3} \alpha^{\text{spl}}_k f_k\left(t_{d[i]}\right) + \\
&\qquad \beta^{\text{geno}}_{g[i]} + \beta^{\text{sex}}_{s[i]} + \beta^{\text{strain}}_{j[i]} + \beta^{\text{inv}}_{v[i]} + \beta^{\text{meta}}_{m[i]} + \sum_{p=1}^{3} \beta^{\text{poly}}_p t^p_{d[i]} \\
\alpha^{\text{day}}_d \mid \sigma^2_{\text{day}} &\sim N\left(0,\ \sigma^2_{\text{day}}\right),\ \text{for } d = 1, \ldots, D \\
\alpha^{\text{litter}}_l \mid \sigma^2_{\text{litter}} &\sim N\left(0,\ \sigma^2_{\text{litter}}\right),\ \text{for } l = 1, \ldots, L \\
\alpha^{\text{spl}}_k \mid \sigma^2_{\text{spl}} &\sim N\left(0,\ \sigma^2_{\text{spl}}\right),\ \text{for } k = 1, \ldots, K
\end{aligned}
$$

where g indexes genotype, s sex, j strain, v investigator, and m metadata group; t_d is the time point corresponding to the dth day. The functions $f_k(\cdot)$ denote basis functions of a B-spline basis for a cubic spline with knots at regularly spaced quantiles of the empirical distribution of days, and the number of knots, K, rounded down from the number of unique days divided by 10.

Non-informative priors were specified for β and σ^2 within the conjugate prior families available in the software package used (MCMCglmm [2, 3]). The location parameters β were allocated independent Normal(mean = 0, variance = 100) priors.[1] The variance parame-

[1] The variance (= 100) of the diffuse Normal prior on the location parameters was chosen to allow large parameter values in the context of the data having been scaled to unit standard deviation prior to analysis (as here). The posterior is insensitive to the particular choice of large variance, provided it is large enough (e.g. varying the parameter from 100 to 10000 would lead to a similar posterior).

ters σ^2 were allocated independent Inverse-gamma(shape = 0.01, rate = 0.01) priors.[2]

For computational speed when fitting the model to multiple permuted data sets, a two-stage model fitting procedure was implemented (Appendix A).

III.1.2 Analysis of categorical phenotypes

Categorical phenotypes, including those with more than two levels, were dichotomized into reference[3] ($y_i = 0$) and non-reference categories ($y_i = 1$) and were analysed under a multilevel over-dispersed logistic regression model with parameters for litter (α^{litter}), genotype (β^{geno}), sex (β^{sex}), strain (β^{strain}), investigator (β^{inv}) and metadata group (β^{meta}). Litter effects were modelled hierarchically with variance component σ^2_{litter}. The inclusion of residuals, denoted by α^{resid}, provide an overdispersed logistic model that is the default in the software package used (MCMCglmm [2, 3]). For any particular mutant line, the following model was fitted only to data from that mutant line along with data from all baseline animals phenotyped in the same centre:

$$\begin{aligned}
\Pr(y_i = 1) &= \text{logit}^{-1}\left(\alpha^{\text{litter}}_{l[i]} + \alpha^{\text{resid}}_i + \beta^{\text{geno}}_{g[i]} + \beta^{\text{sex}}_{s[i]} + \beta^{\text{strain}}_{j[i]} + \beta^{\text{inv}}_{v[i]} + \beta^{\text{meta}}_{m[i]}\right) \\
\alpha^{\text{litter}}_l \mid \sigma^2_{\text{litter}} &\sim N\left(0,\ \sigma^2_{\text{litter}}\right), \text{ for } l = 1, \ldots, L \\
\alpha^{\text{resid}}_i &\sim N(0,\ 1)
\end{aligned}$$

The location parameters β were allocated weakly informative, independent Normal(0, 25) priors, motivated by the considerations outlined in [5] and its references.[4] The litter variance parameter σ^2_{litter}, modelling covariance between binary observations within a litter, was allocated an Inverse-gamma(0.8, 0.04) empirical Bayes-type prior.[5] For computational speed when fitting the model to multiple permuted data sets, a two-stage model fitting procedure was implemented (Appendix A).

III.1.3 Control of the false discovery rate (FDR)

To quantify the evidence in favour of a non-zero genotype effect for any particular (centre, phenotype, mutant line) combination, we used the following posterior summary statistic:

$$T := 2 \times \min\left\{\Pr(\beta^{\text{geno}} \leq 0 \mid y),\ \Pr(\beta^{\text{geno}} \geq 0 \mid y)\right\}\ . \tag{1}$$

[2] A non-informative Inverse-gamma(ε, ε) prior with small ε is a common but pragmatic choice for variance components, and we were guided by what was available in the software package used. It is known that there can be a degree of posterior sensitivity to the particular choice of ε (e.g. as ε varies from 0.01 to 0.001) [4]. In future methods development we would prefer a non-informative half-Cauchy prior as suggested by [4].

[3] The one or more categories pooled into a particular reference class represent the typical characteristics of baseline animals, and were selected through discussion with domain experts.

[4] In [5], a Cauchy distribution with scale parameter 2.5 was suggested as a weakly informative default prior for the logistic model, with its relevant properties being that it "gives preference to values less than 5, with the Cauchy allowing the occasional possibility of very large values." Our choice of prior was restricted to be Gaussian in the software used, so we approximated the distribution suggested in [5] by selecting a Normal(0, variance = 25), i.e. with scale parameter 5, which places 68% of mass within the interval $[-5, 5]$ while admitting very large (up to about 15) absolute values on log odds scale.

[5] The rationale for this empirical-Bayes prior is to share information across phenotypes and centres on the litter covariance effect. The prior will have largest effect on the posterior, and corresponding benefit to inference relative to a non-informative prior, at phenotypes where very little information about the litter covariance effect is available, e.g. when most or all of the observations on baseline animals fall into the same category. The hyperparameters (shape = 0.8, rate = 0.04) were selected by maximum likelihood so that the empirical-Bayes prior matched the empirical distribution of estimates of σ^2_{litter} from across all centres and parameters obtained under a non-informative Inverse-gamma(0.01, 0.01) prior.

Each (centre, phenotype, mutant line) combination was annotated if

$$T_{(\text{cen,phen,line})} < \tau_{(\text{cen,phen})} \,. \tag{2}$$

The (centre, phenotype)-specific threshold $\tau_{(\text{cen,phen})}$ was selected to control the FDR.

The FDR was estimated by permutations in which, for each (centre, phenotype, mutant line) combination, $P = 10$ negative-control instances of the mutant line's data were generated by randomly relabelling baseline data from the same centre. Multiple sets of 10 permutations were used to estimate the FDR; e.g. (centre, phenotype)-specific FDR was estimated, as described in (3) below, using permutations generated from all genes – 10 per gene – at that (centre, phenotype), so that the median number of permutations contributing to a (centre, phenotype) FDR estimate was 920 (interquartile range 650-1400).

The permutation approach was designed to mimic relevant characteristics of the mutant's data structure in the relabelled baseline data, and is described in Appendix B.

With the πth permutation for a (centre, phenotype, mutant line) combination yielding $T^{(\pi)}_{(\text{cen,phen,line})}$, the FDR at a particular (centre, phenotype) combination was estimated as

$$\begin{aligned} \widehat{FDR}_{(\text{cen,phen})} &= \frac{\text{Estimated number of false annotations}}{\text{Number of annotations}} \\ &= \frac{\sum_{\text{line}} \frac{1}{P} \sum_{\pi=1}^{P} I\left[T^{(\pi)}_{(\text{cen,phen,line})} < \tau_{(\text{cen,phen})}\right]}{\sum_{\text{line}} I\left[T_{(\text{cen,phen,line})} < \tau_{(\text{cen,phen})}\right]} \end{aligned} \tag{3}$$

with $\widehat{FDR}_{(\text{cen,phen})}$ defined to be zero when the denominator was zero, and where $I[\cdot]$ denotes the indicator function. The global FDR across all centres and phenotypes was estimated similarly as

$$\widehat{FDR} = \frac{\sum_{\text{cen}} \sum_{\text{phen}} \sum_{\text{line}} \frac{1}{P} \sum_{\pi=1}^{P} I\left[T^{(\pi)}_{(\text{cen,phen,line})} < \tau_{(\text{cen,phen})}\right]}{\sum_{\text{cen}} \sum_{\text{phen}} \sum_{\text{line}} I\left[T_{(\text{cen,phen,line})} < \tau_{(\text{cen,phen})}\right]} \tag{4}$$

Initially a single threshold $\tau_{\max} = 10^{-4}$ was found that controlled the global FDR at 5%, i.e. such that, in (4), $\widehat{FDR} < 0.05$ when all $\tau_{(\text{cen,phen})} \equiv \tau_{\max}$. The (centre, phenotype)-specific thresholds were then chosen to control each $\widehat{FDR}_{(\text{cen,phen})} < 0.05$, under the constraint that the (centre, phenotype)-specific thresholds must be at least as stringent as the global threshold, i.e. $\tau_{(\text{cen,phen})} \leq \tau_{\max}$.[6]

III.1.4 Power and experimental design

Power calculations were performed to investigate and compare various designs for phenotyping pipelines. Design variables included: the number of litters of each mutant line phenotyped, whether litters were split across days, whether baseline animals accompanied mutant animals (i.e. were phenotyped on the same day) and how many baseline litters were phenotyped per day. Realistic correlation structure was introduced into the model using the estimated proportions of variance attributed to day, litter and residual components, averaged across phenotypes measured within a particular procedure; e.g. for

[6] The estimators $\widehat{FDR}_{(\text{cen,phen})}$ can be imprecise, and so the constraint $\tau_{(\text{cen,phen})} \leq \tau_{\max}$ was enforced for all (centre, phenotype) combinations to protect against choice of unsuitably large (i.e. not stringent enough) thresholds in instances of underestimation of the true FDR.

Calorimetry the average estimated variance proportions were $\nu_{\text{day}} = 0.21$, $\nu_{\text{litter}} = 0.08$ and $\nu_{\text{resid}} = 0.71$.

Inference for power calculations was performed under a frequentist linear model with correlation matrix for the residuals (generalized least squares), $\boldsymbol{R}$, specified from estimated variance proportions ν_{day}, ν_{litter} and ν_{resid}:

$$\begin{aligned} \boldsymbol{y} &\sim N(\boldsymbol{X}\boldsymbol{\beta}^{\text{geno}}, \boldsymbol{R}\sigma^2) \\ \boldsymbol{R} &= \boldsymbol{Z}_{\text{day}}\boldsymbol{Z}_{\text{day}}^T\nu_{\text{day}} + \boldsymbol{Z}_{\text{litter}}\boldsymbol{Z}_{\text{litter}}^T\nu_{\text{litter}} + \boldsymbol{I}\nu_{\text{resid}} \end{aligned}$$

where the $\boldsymbol{Z}$ are design matrices relating $\boldsymbol{y}$ to day and litter, and $\boldsymbol{X}$ relates $\boldsymbol{y}$ to genotype. Detectable effect size was determined based on the test of the null hypothesis of no genotypic effect using the standard t-statistic under its asymptotic Gaussian distribution[7] at a significance level of 10^{-7} and with power 80%. A significance level of 10^{-7} was found to control the global FDR at 5% in a permutation analysis of the EUMODIC data, performed as described in section "Control of the false discovery rate (FDR)" above, but with $T_{(\text{cen,phen,line})}$ and $\tau_{(\text{cen,phen})}$ now corresponding to p-value and significance level respectively under a frequentist linear mixed-effects model (with day and litter as random effects and genotype, sex, strain, and metadata group as fixed effects). Detectable standardized effect size is presented, i.e.

$$d = \frac{\left|\beta_{\text{mut}}^{\text{geno}} - \beta_{\text{bas}}^{\text{geno}}\right|}{\sigma} .$$

The experimental design and analysis for the EUMODIC project had the following properties (note that both sexes are included in the numbers below):

1. 68% of mutant lines were phenotyped across more than one day;
2. 71% of mutant days were accompanied by baseline animals;
3. all centre-specific baseline data were included in the analysis;
4. the average numbers of mutant and baseline animals per litter were 2.5 and 2.7 respectively (we use 2 as the default in the power calculation, as described below);
5. the average number of mutant animals of each line was 16.4 (we use 14 [7 litters of size 2] for the default, described below);
6. the average numbers of mutant and baseline animals phenotyped per day were 7.1 and 5.7 respectively (we use 4 per day as the default for the power calculations, described below [2 litters of size 2 per day]);
7. On average, mutant lines were compared to 119 days' worth of baseline animals, and 97% of mutant lines were compared to at least 50 days worth.

The values of the experimental design and analytical variables used in power calculations are listed below; note that the underlined choices indicate those values representative of the typical design and analysis used in the EUMODIC project and which were just described above.[8]

1. Whether all mutant litters are phenotyped on a single day, or each on a different day
    - Single day

[7] This is a reasonable approximation as the combined baseline/mutant sample sizes are sufficiently high; in particular there are always at least 54 animals in the power calculations performed

[8] The underlined choices do not completely coincide with the most powerful design considered in the power calculations: the design with mutants accompanied on a single day was marginally more powerful than the design having mutants accompanied on multiple days, though the latter design has other advantages, such as being relatively robust to an unplanned absence of accompanying controls.

- Multiple days, with two mutant litters per day

2. Whether mutants are accompanied (i.e. whether baseline animals are phenotyped on the same day(s))
   - Accompanied
   - Not accompanied
3. Whether all baseline data are analysed
   - Include all baseline data in analysis
   - Include just accompanying baseline data
4. Number of animals in a litter $\in \{2\}$
5. Number of mutant litters phenotyped $\in \{2, 3, 4, 5, 6, 7, 8, 9, 10, 11, 12\}$
6. Number of baseline litters per day $\in \{1, 2, 3\}$
7. Total number of baseline days $\in \{50, 100, 200\}$

III.1.5 Appendix A – Model fitting

Evaluating the posterior for the mutant genotype effect proceeded in two stages. In the first stage, thinned samples, $\boldsymbol{\theta}_{\text{bas}}^{(1)}, \ldots, \boldsymbol{\theta}_{\text{bas}}^{(K)}$, were drawn from the posterior distribution $p(\boldsymbol{\theta}_{\text{bas}} \mid \boldsymbol{y}_{\text{bas}})$ using MCMC as implemented in the R package MCMCglmm [2, 3], where $\boldsymbol{\theta}_{\text{bas}}$ denotes all $\boldsymbol{\beta}$ and $\boldsymbol{\sigma}$ parameters in the (quantitative or categorical) model apart from the mutant genotype parameter, i.e. $\boldsymbol{\theta}_{\text{bas}} \equiv \{\boldsymbol{\beta}, \boldsymbol{\sigma}\} \setminus \beta_{\text{mut}}^{\text{geno}}$.

In the second stage, performed separately for each mutant line, the marginal posterior for the mutant genotype effect, $\theta_{\text{mut}} \equiv \beta_{\text{mut}}^{\text{geno}} - \beta_{\text{bas}}^{\text{geno}}$, conditional on baseline and that mutant's data, $p(\theta_{\text{mut}} \mid \boldsymbol{y}_{\text{bas}}, \boldsymbol{y}_{\text{mut}})$, was evaluated via numerical integration methods, as follows. By Bayes' theorem,

$$\begin{aligned} p(\theta_{\text{mut}} \mid \boldsymbol{y}_{\text{mut}}, \boldsymbol{y}_{\text{bas}}) &\propto p(\boldsymbol{y}_{\text{mut}} \mid \theta_{\text{mut}}, \boldsymbol{y}_{\text{bas}}) p(\theta_{\text{mut}} \mid \boldsymbol{y}_{\text{bas}}) \\ &= p(\boldsymbol{y}_{\text{mut}} \mid \theta_{\text{mut}}, \boldsymbol{y}_{\text{bas}}) p(\theta_{\text{mut}}) \,, \end{aligned} \tag{5}$$

where (5) used $\theta_{\text{mut}} \perp\!\!\!\perp \boldsymbol{y}_{\text{bas}}$.[9] The first term in (5) was estimated by Monte Carlo integration using the draws from the posterior $p(\boldsymbol{\theta}_{\text{bas}} \mid \boldsymbol{y}_{\text{bas}})$ obtained in stage one:

$$\begin{aligned} p(\boldsymbol{y}_{\text{mut}} \mid \theta_{\text{mut}}, \boldsymbol{y}_{\text{bas}}) &= \int p(\boldsymbol{y}_{\text{mut}} \mid \theta_{\text{mut}}, \boldsymbol{y}_{\text{bas}}, \boldsymbol{\theta}_{\text{bas}}) p(\boldsymbol{\theta}_{\text{bas}} \mid \theta_{\text{mut}}, \boldsymbol{y}_{\text{bas}}) \, \mathrm{d}\boldsymbol{\theta}_{\text{bas}} \\ &= \int \frac{p(\boldsymbol{y}_{\text{mut}}, \boldsymbol{y}_{\text{bas}} \mid \theta_{\text{mut}}, \boldsymbol{\theta}_{\text{bas}})}{p(\boldsymbol{y}_{\text{bas}} \mid \theta_{\text{mut}}, \boldsymbol{\theta}_{\text{bas}})} p(\boldsymbol{\theta}_{\text{bas}} \mid \boldsymbol{y}_{\text{bas}}) \, \mathrm{d}\boldsymbol{\theta}_{\text{bas}} \qquad (6) \\ &\approx \frac{1}{K} \sum_{k=1}^{K} \frac{p(\boldsymbol{y}_{\text{mut}}, \boldsymbol{y}_{\text{bas}} \mid \theta_{\text{mut}}, \boldsymbol{\theta}_{\text{bas}}^{(k)})}{p(\boldsymbol{y}_{\text{bas}} \mid \boldsymbol{\theta}_{\text{bas}}^{(k)})} \qquad (7) \end{aligned}$$

where (6) used $\boldsymbol{\theta}_{\text{bas}} \perp\!\!\!\perp \theta_{\text{mut}} \mid \boldsymbol{y}_{\text{bas}}$, and (7) used $\boldsymbol{y}_{\text{bas}} \perp\!\!\!\perp \theta_{\text{mut}} \mid \boldsymbol{\theta}_{\text{bas}}$. In the categorical model, evaluating the numerator and denominator in the summand of (7) required numerical integration, performed using Gauss-Hermite quadrature, to marginalise with respect to the random effects, $\boldsymbol{\alpha}^{\text{day}}$ and/or $\boldsymbol{\alpha}^{\text{litter}}$.[10] Finally, (7) was substituted in (5) and the

[9] We use the notation $x \perp\!\!\!\perp y \mid z$ to denote conditional independence of x and y given z.

[10] For the quantitative response model, the spline random effects were included in $\boldsymbol{\theta}_{\text{bas}}$, i.e. $\boldsymbol{\theta}_{\text{bas}} \equiv \{\boldsymbol{\beta}, \boldsymbol{\sigma}, \boldsymbol{\alpha}^{\text{spl}}\} \setminus \beta_{\text{mut}}^{\text{geno}}$.

posterior's normalising constant calculated via integration with respect to θ_{mut} using the trapezoidal rule.

Numerical integration for logistic-response model: without a day effect in the categorical model, $\boldsymbol{y}_{\text{mut}}$ and $\boldsymbol{y}_{\text{bas}}$ are conditionally independent given $(\theta_{\text{mut}}, \boldsymbol{\theta}_{\text{bas}}^{(k)})$, so the formula in (7) can be expressed as

$$\begin{aligned}\frac{1}{K}\sum_{k=1}^{K}\frac{p(\boldsymbol{y}_{\text{mut}}, \boldsymbol{y}_{\text{bas}} \mid \theta_{\text{mut}}, \boldsymbol{\theta}_{\text{bas}}^{(k)})}{p(\boldsymbol{y}_{\text{bas}} \mid \boldsymbol{\theta}_{\text{bas}}^{(k)})} &= \frac{1}{K}\sum_{k=1}^{K}\frac{p(\boldsymbol{y}_{\text{mut}}, \mid \theta_{\text{mut}}, \boldsymbol{\theta}_{\text{bas}}^{(k)})p(\boldsymbol{y}_{\text{bas}} \mid \boldsymbol{\theta}_{\text{bas}}^{(k)})}{p(\boldsymbol{y}_{\text{bas}} \mid \boldsymbol{\theta}_{\text{bas}}^{(k)})} \\ &= \frac{1}{K}\sum_{k=1}^{K} p(\boldsymbol{y}_{\text{mut}}, \mid \theta_{\text{mut}}, \boldsymbol{\theta}_{\text{bas}}^{(k)})\end{aligned}$$

and

$$\begin{aligned}p(\boldsymbol{y}_{\text{mut}}, \mid \theta_{\text{mut}}, \boldsymbol{\theta}_{\text{bas}}^{(k)}) &= \int\int p(\boldsymbol{y}_{\text{mut}} \mid \theta_{\text{mut}}, \boldsymbol{\theta}_{\text{bas}}^{(k)}, \boldsymbol{\alpha}^{\text{litter}}, \boldsymbol{\alpha}^{\text{resid}})p(\boldsymbol{\alpha}^{\text{litter}}, \boldsymbol{\alpha}^{\text{resid}} \mid \boldsymbol{\sigma}^{(k)})\,\mathrm{d}\boldsymbol{\alpha}^{\text{litter}}\,\mathrm{d}\boldsymbol{\alpha}^{\text{resid}} \\ &= \prod_{l=1}^{L}\int\left[\prod_{i=1}^{N_l}\int g_{li}(\alpha_l^{\text{litter}}, \alpha_{li}^{\text{resid}})\;\; p(\boldsymbol{\alpha}_{li}^{\text{resid}} \mid \sigma_{\text{resid}}^{(k)})\,\mathrm{d}\alpha_{li}^{\text{resid}}\right] p(\alpha_l^{\text{litter}} \mid \sigma_{\text{litter}}^{(k)})\,\mathrm{d}\alpha_l^{\text{litter}}\end{aligned}$$

where

$$\begin{aligned}g_{li}(\alpha_l^{\text{litter}}, \alpha_{li}^{\text{resid}}) &:= p(y_{\text{mut},li} \mid \theta_{\text{mut}}, \boldsymbol{\theta}_{\text{bas}}^{(k)}, \alpha_l^{\text{litter}}, \alpha_{li}^{\text{resid}}) \\ &= \frac{\exp\left(\boldsymbol{x}_{li}^T\boldsymbol{\beta}^{(\boldsymbol{k})} + \beta_{\text{mut}}^{\text{geno}} + \alpha_l^{\text{litter}} + \alpha_{li}^{\text{resid}}\right)^{y_{\text{mut},li}}}{1 + \exp\left(\boldsymbol{x}_{li}^T\boldsymbol{\beta}^{(\boldsymbol{k})} + \beta_{\text{mut}}^{\text{geno}} + \alpha_l^{\text{litter}} + \alpha_{li}^{\text{resid}}\right)}\,.\end{aligned}$$

The integrals were performed using Gauss-Hermite quadrature, e.g.

$$\begin{aligned}\int_{-\infty}^{\infty} g(\alpha)p(\alpha \mid \sigma)\,\mathrm{d}\alpha &= \int_{-\infty}^{\infty} g(\alpha)\frac{1}{\sqrt{2\pi\sigma^2}}\exp\left(-\frac{\alpha^2}{2\sigma^2}\right)\mathrm{d}\alpha \\ &= \int_{-\infty}^{\infty} g(\alpha\sqrt{2\sigma^2})\frac{1}{\sqrt{\pi}}\exp\left(-\alpha^2\right)\mathrm{d}\alpha \\ &\approx \frac{1}{\sqrt{\pi}}\sum_{i=1}^{n} w_i g(z_i\sqrt{2\sigma^2})\,,\end{aligned}$$

where the z_i and w_i are the are the roots and weights of the Hermite polynomial $H_n(\cdot)$.

III.1.6 Appendix B – Permutation scheme

For the purposes of estimating and controlling the false discovery rate among phenotype calls, baseline data were relabelled to create synthetic null mutant data and analysed similarly to the true mutant data. So as to attain accurate FDR estimates, synthetic mutants were sampled from baseline animals in such a way as to match closely the experimental design implemented for true mutants. Design variables desirable to match across synthetic and true mutants included: the number of mutant animals, the number of mutant litters, the number of days across which phenotyping occurred, whether or not baseline animals were phenotyped on the same day, and the calendar time points at which phenotyping occurred.

For each (centre, phenotype, mutant line) combination, several synthetic null mutant data sets were independently sampled, each matching the design characteristics of that particular true mutant data set. A mutant data set comprised one or more *mutant days*, each

comprising mutant data gathered on a single day. For each mutant day of a true mutant data set, a *baseline day*, comprising all baseline data gathered on a single day, was chosen and relabelled to create a corresponding synthetic null mutant day.

The following notation is used to describe the scheme for sampling baseline days:

d_{mut} : the date of the mutant day (in days since arbitrary reference date)
l_{mut} : the number of mutant litters phenotyped on the mutant day
δ_{mut} : indicator whether mutants were *accompanied*[a] ($\delta_{\text{mut}} = 1$) or not ($\delta_{\text{mut}} = 0$)
B : the total number of baseline days
d_i : the date of the ith baseline day ($i = 1, \ldots, B$)
l_i : number of baseline litters phenotyped on the ith baseline day ($i = 1, \ldots, B$)

[a] Mutants on a particular mutant day were *accompanied* if baseline animals were also phenotyped on that date.

The (unnormalized) sampling distribution was:

$$\Pr(\text{select } i\text{th baseline day}) \propto t_2\left(\frac{d_i - d_{\text{mut}}}{14}\right) I[l_i \geq l_{\text{mut}} + \delta_{\text{mut}}] \tag{8}$$

where $t_2(\cdot)$ denotes the density function of the Student t_2 distribution, and $I[\cdot]$ denotes the indicator function. The t_2 distribution and scaling in units of 14 days were heuristically selected with particular attention to the trade-off between close temporal matching and conditional independence of multiple synthetic data sets.

Once a baseline day had been selected, l_{mut} of that day's litters were relabelled as mutant litters, and its remaining data were either retained without relabelling if $\delta_{\text{mut}} = 1$, or were discarded if $\delta_{\text{mut}} = 0$. In creating a particular instance of a synthetic mutant data set comprising multiple mutant days, sampling of baseline days was performed without replacement.

III.1.7 SI References

[1] Ruppert, D., Wand, M. P., and Carroll, R. J. *Semiparametric Regression*. Cambridge Series in Statistical and Probabilistic Mathematics. Cambridge University Press, first edition, (2003).

[2] Hadfield, J. D. *Journal of Statistical Software* **33**(2), 1–22 February (2010).

[3] R Development Core Team. *R: A Language and Environment for Statistical Computing*. R Foundation for Statistical Computing, Vienna, Austria, (2010).

[4] Gelman, A. *Bayesian Analysis* **1**(3), 515–533 (2006).

[5] Gelman, A., Jakulin, A., Grazia Pittau, M., and Su, Y.-S. *The Annals of Applied Statistics* **2**(4), 1360–1383 (2008).

III.2 The EUMODIC Consortium

Universitat Autònoma Barcelona (UAB), Spain
Fatima Bosch [1]
Jesús Ruberte [1]
Tura Ferre [1]
Anna Pujol [1]
Pedro Otaegui [1]
Sylvie Franckhauser [1]
David Ramos [1]
Miquel Garcia [1]

Ani.Rhône-Alpes Lyon, France
Jacqueline Marvel [2]
Veronique Queste [2]
Romain Dacquin [2]
Sophia Djebali [2]
Pierre Jurdic [2]

Biomedical Sciences Research Center 'Alexander Fleming' Athens, Greece
George Kollias [3]
Christina Chandras [3]
Eleni Douni [3]
Vassilis Aidinis [3]
Dimitris Kontoyiannis[3]
Maria Kamber[3]

CNIO Madrid, Spain
Mariano Barbacid [4]
Carmen Guerra [4]
Marta Cañamero [4]
Pierre Dubus [5]

CNR, IBC Monterotondo, Italy
Glauco Tocchini-Valentini [6]
Silvia Mandillo [6]
Elisabetta Golini [6]
Daniela Marazziti [6]
Giancarlo Deidda [6]

CNR, IBC (cont.)
Nicoletta Rossi [6]
Brendan Doe [6]
Rafaele Matteoni [6]
Marcello Raspa [6]
Alessia Gambadoro [6]
Francesco Chiani [6]
Ferdinando Scavizzi [6]
Richard Hugh Butler [6]
Gianfranco Di Segni [6]
Paolo Fruscoloni [6]
Patrizia Calandra [6]
Cecilia Mannironi [6]
Daniela Scarabino [6]
Giuseppe D. Tocchini-Valentini [6]
Michela Zamboni [6]
Sabrina Putti [6]
Chiara Di Pietro [6]
Serena Gastaldi [6]

CNRS TAAM UPS44 – INEM UMR, France
Yann Hérault [7]
Bernard Ryffel [7]
Valérie Quesniaux [7]
Isabelle Couillin [7]
François Erard [7]
Marc le Bert [7]
Jacques Lignon [7]
Florence Savigny [7]
Isabelle Maillet-Mercier [7]
Stéphanie Rose [7]
Rachel Vacher [7]
Léa Brault [7]
Patricia Lopes Pereirea [7]
Véronique Brault [7]
Emilie Dalloneau [7]
Stéphanie Pothion [7]
Alexandre Diet [7]
Cécile Fremond [7]

EMBL Mouse Biology Unit Monterotondo, Italy
Nadia Rosenthal [8]
Mumna Al Banchaabouchi [8]
Raffaele Migliozzi [8]
Ekaterina Salimova [8]

Helmholtz Centre for Infection Research (HZI), Braunschweig, Germany
Bastian Pasche [9]
Fabio Pisano [9]
Silke Bergmann [9]
Werner Müller [10]
Andreas Lengeling [11]

Helmholtz Zentrum München German Research Center for Environmental Health Munich (HMGU), Germany
Martin Hrabě de Angelis [12, a]
Valérie Gailus-Durner [12]
Helmut Fuchs [12]
Thure Adler [12, 14]
Antonio Aguilar-Pimentel [12, b]
Lore Becker [12, c]
Raffi Bekeredjian [12, d]
Dirk H. Busch [9]
Julia Calzada-Wack [e]
Oliver Eickelberg [g]
Irene Esposito [e]
Jack Favor [f]
Lilian Garrett [13]
Lisa Glasl [13]
Alexander Götz [g]
Jochen Graw [13]
Wolfgang Hans [12]
Heinz Höfler [e]
Sabine M. Hölter [13]
Anja Hurt [12]
Boris Ivandic [12, d]
Hugo A. Katus [12, d]
Martin Klingenspor [12, h]
Thomas Klopstock [12, c]
Christoph Lengger [12]
Tonia Ludwig [12]
Holger Maier [12]
Susan Marschall [12]
Kateryna Micklich [12]

HMGU (cont.)
Beatrix Naton [12]
Frauke Neff [e]
Markus Ollert [12, b]
Natalia Pellegata [e]
Oliver Puk [13]
Leticia Quintanilla-Fend [e]
Ildiko Racz [12, i]
Birgit Rathkolb [12, j]
Jan Rozman [12, h]
Karl-Heinz Schäble [12]
Evelyn Schiller [12]
Anja Schrewe [12]
Holger Schulz [g]
Ralf Steinkamp [12]
Claudia Stöger [12]
Tobias Stöger [g]
Minxuan Sun [13]
Monica Tost [e]
Irina Treise [12]
Daniela Vogt-Weisenhorn [13]
Monja Willershäuser [12]
Eckhard Wolf [j,12]
Annemarie Wolff-Muscate [13]
Wolfgang Wurst [13, k,l,m]
Ali Önder Yildirim [g]
Ramona Zeh [12]
Andreas Zimmer [12, i]

Institut Clinique de la Souris (IGBMC), Strasbourg, France
Jean-Louis Mandel [15]
Yann Hérault [15]
Tania Sorg [15]
Mohammed Selloum [15]
Abdel Ayadi [15]
Guillaume Pavlovic [15]
Marie-Christine Birling [15]
Laurent Monassier [15]
Michel Roux [15]
Manuel Mark [15]
Dalila Ali-Hadji [15]
Philippe André [15]
Elodie Bedu [15]
Julien Becker [15]
Benoit Petit-Demoulière[15]
Marie-France Champy [15]
Philippe Charles [15]

IGBMC (cont.)
Roy Combe [15]
André Dierich [15]
Isabelle Goncalves Da Cruz [15]
Sylvie Jacquot [15]
Hughes Jacobs [15]
Sophie Leblanc [15]
Hamid Meziane [15]
Laurent Vasseur [15]
Olivia Wendling [15]
Gregory Amann[15]
Aurelie Auburtin[15]
Lahcen El Fertak[15]
Alain Guimond[15]
Patrice Goetz[15]
Valerie Lalanne[15]
Elise le Marchand[15]
Stéphanie Muller[15]
Aline Lux[15]
Christophe Mittelhauser[15]
Laurent Pouilly[15]
David Moulaert[15]
Emilie Peter[15]
Fabrice Riet[15]
Stephane Rousseau[15]
Isabelle Tilly[15]
Christelle Wagner[15]
Bruno Weber[15]
Anne Wolter[15]
Véronique Brault [15]
Claire Chevalier [15]
Arnaud Duchon [15]
Emilie Dalloneau [15]
Emilie Velot [15]

MRC Harwell, UK
Steve Brown [16]
Hilary Gates [16]
Niels Adams [17]
Sarah Atkins [16]
Tim Beck [16]
Kathryn Birch [17]
Andy Blake [16]
Debra Brooker [16]
Heather Cater [17]
Kan Pai Chiev [16]
Andre Chouankam [16]
Roger Cox [16]

MRC Harwell (cont.)
Paul Denny [16]
Irina Emelyanova [16]
Martin Fray [17]
George Gkoutos [30]
Simon Greenaway [16]
Ahmad Hassan [16]
John Hancock [16]
Tertius Hough [17]
Kelly Hunt [16]
Elizabeth Joynson [17]
Rachel Kendall [16]
Sharon Kitchen [17]
Ramakrishna Kurapati [16]
Heena Lad [16]
Kirsty Lee [16]
Dee Lynch [17]
Ann-Marie Mallon [16]
Hugh Morgan [16]
Helen Natukunda [17]
George Nicholson [29]
Pat Nolan [16]
Viral Panchal [16]
Paras Pathak [17]
Amanda Pickard [17]
Paul Potter [17]
Deen Quwailid [16]
Matthew Reddon [16]
Ahmad Retha [16]
Luis Santos [16]
Michelle Simon [16]
Anne Southwell [16]
Michelle Stewart [17]
Lydia Teboul [17]
Adele Traynor [16]
Simon Vowell [16]
Jane Vowles [17]
Alison Walling [17]
Tom Weaver [17]
Sara Wells [17]
Henrik Westerberg [16]
Debbie Williams [16]
Joe Wood [17]
Rumana Zaman [16]

MRC Human Genetics Unit
Edinburgh, UK
Ian Jackson [18]
Sally Cross [18]
Russell Joynson [18/17]
Shalini Jadeja [18]
Lisa McKie [18]

Tel Aviv University
Israel
Karen B. Avraham [19]
Amiel Dror [19]
Shaked Shivatzki [19]
Anya Rudnicki [19]
Danielle Lenz [19]
Tal Elkan [19]
Zippora Brownstein [19]

Telethon Institute of Genetics and Medicine (TIGEM)
Italy
Andrea Ballabio [20]
Graciana Diez-Roux [20]

The Roslin Institute, UK
Andreas Lengeling[21]

University of Cambridge
UK
Paul Schofield [22]
Michael Gruenberger [22]
Julian L Griffin [28]

University of Lausanne, Switzerland
Walter Wahli [24]
Frederic Preitner [24]
Mehdi Tafti [24]
Bernard Thorens [24]
Béatrice Desvergne [24]
Liliane Michalik [24]
Salima Metref [24]
Anabela Da Costa [24]
Paul Franken [24]
Yann Emmenegger [24]

University of Manchester, UK
Ludwig Neyses [25]
Elizabeth Cartwright [26]
Sukhpal Prehar [26]
Min Zi [26]

The Wellcome Trust Sanger Institute (WTSI), Cambridge, UK
Jacqueline K White [27]
Ramiro Ramirez-Solis [27]
Anna-Karin Gerdin [27]
Natasha A Karp [27]
James N Bussell [27]
Jennifer Salisbury [27]
Ed Ryder [27]
Christine Podrini [27]
Richard Houghton [27]
Jeanne Estabel [27]
Joanna Bottomley [27]
David Richardson [27]
David G Melvin [27]
David Sunter [27]
Niels C Adams [27]
David J Adams [27]
Karen P Steel [27]
Emma Cambridge [27]
Caroline Barnes [27]
Damian Carragher [27]
Prabhjoat Chana [27]
Jing Chen [27]
Kay Clarke [27]
Yvette Hooks [27]
Natalia Igosheva [27]
Neil Ingham [27]
Ozama Ismail [27]
Hannah Jackson [27]
Leanne Kane [27]
Rosalind Lacey [27]
David Tino Lafont [27]
Mark Lucas [27]
Simon Maguire [27]
Katherine McGill [27]
Rebecca McIntyre [27]
Lynda Mottram [27]
Lee Mulderrig [27]
Selina Pearson [27]

WTSI (cont.)
Hayley J Protheroe [27]
Laura-Anne Roberson [27]
Grace Salsbury [27]
Mark Sanderson [27]
Daniel Sanger [27]
Carl Shannon [27]
Elizabeth Tuck [27]
Valerie E Vancollie [27]
Sophie Messager [27]
Ryan Beveridge [27]
Lauren Baker [27]
Diane Gleeson [27]
Ross Cook [27]
Matt Hardy [27]
Kifayathullah Liakath Ali [27]
Stacey Price [27]
Debarati Sethi [27]
Elizabeth Trenchard [27]
Sapna Vyas [27]
Elizabeth Wynn [27]
Lisa Brackenbury [27]
Arthur Evans [27]
David Gannon [27]
Mark Griffiths [27]
Simon Holroyd [27]
Christian Kipp [27]
Wei Li [27]
Helen Tharagonnet [27]
Chukwuma Agu [27]
Jackie Bryant [27]
Liz Delaney [27]
Ellen Brown [27]
Adam Collinson [27]
Evelyn Grau [27]
Catherine Ingle [27]
Helen Kundi [27]
Alla Madich [27]
Danielle Mayhew [27]
Tom Metcalf [27]
Stuart Newman [27]
Johanna Pass [27]
Laila Pearson [27]
Caroline Sinclair [27]
Hannah Wardle-Jones [27]
Michael Woods [27]
Sarah Harrison [27]
James Harrison [27]
Charles-Etienne Dumeau [27]

WTSI (cont.)
Helen Reynolds [27]
Daniel Biggs [27]
Francesca Flack [27]
Gemma White [27]
Terry Brown [27]
Andrea Kirton [27]
Liam Alexander [27]
Claire Rogerson [27]
Jordan McDermott [27]
Nicola Griggs [27]
Silvia Hrnciarova [27]
Pawel Zielezinski [27]

EUMODIC stands for the “European Mouse Disease Clinic: A distributed phenotyping resource for studying human disease”. The EUMODIC project was funded by the European Commission within its FP6 Programme, under the thematic area “Life sciences, genomics and biotechnology for health” contract number LSHG-CT-2006-037188

Further information on the EUMODIC project and consortium can be found on the project website: www.eumodic.org

1 Centre of Animal Biotechnology and Gene Therapy, School of Veterinary Medicine, Autonomous University of Barcelona, 08193 Bellaterra, Spain
2 Ani.Rhone-Alpes, AniRA - UMS3444/US8 Biosciences Gerland-Lyon Sud, 50 Avenue Tony Garnier, 69366 Lyon Cedex 7, France
3 Biomedical Sciences Research Center ‘Alexander Fleming’, Athens, Greece
4 CNIO - Centro Nacional de Investigaciones Oncologicas, Molecular Oncology & Comparative Pathology, Melchor Fernandez Almagro 3, 28029 Madrid, Spain
5 University of Bordeaux, Histology and Molecular Pathology Department, EA2406, 146 Rue Leo Saignat, 33076 Bordeaux, France
6 IBC-CNR, Campus “A.Buzzati-Traverso”, via Ramarini 32 00016 Monterotondo Scalo, Rome, Italy
7 CNRS INEM - UMR7355, 3B rue de la ferollerie 45071 Orleans cedex 2, France
8 EMBL Monterotondo, Mouse Phenotyping Facility, “A.Buzzati-Traverso Campus”, via Ramarini 32, 00015 Monterotondo Scalo, Rome, Italy
9 Institute for Medical Microbiology, Immunology and Hygiene, Technische Universität München, Trogerstrasse 9, 81675 Munich, Germany
10 The University of Manchester, AV Hill Building, Oxford Road, Manchester, M13 9PT, UK
11 The Roslin Institute, University of Edinburgh, Easter Bush Veterinary Research Centre, Roslin, Midlothian, EH25 9RG, UK
12 Helmholtz Zentrum München, German Research Center for Environmental Health, Institute of Experimental Genetics and German Mouse Clinic, Ingolstaedter Landstrasse 1, D- 85764 Neuherberg, Germany
13 Helmholtz Zentrum München, German Research Center for Environmental Health, Institute of Developmental Genetics, Ingolstaedter Landstrasse 1, D-85764 Neuherberg, Germany
14 Institute for Medical Microbiology, Immunology and Hygeine, Technische Universität München, Trogerstrasse 9, 81675 Munich, Germany
15 Institut Clinique de la Souris (ICS), 1 Rue Laurent Fries, BP10142, 67404 Illkirch, Cedex, France
16 Medical Research Council Mammalian Genetics Unit, Harwell, Oxfordshire, OX11 0RD, UK
17 Medical Research Council Mary Lyon Centre, Harwell, Oxfordshire, OX11 0RD, UK
18 Medical Research Council Human Genetics Unit, Comparative and Developmental Genetics Department, Western General Hospital, Crewe Road, Edinburgh, EH4 2XU, UK
19 Department of Human Molecular Genetics and Biochemistry, Sackler Faculty of Medicine, Tel Aviv University, Tel Aviv 69978, Israel
20 Telethon Institute of Genetics and Medicine, Via Pietro Castellino 111, 80131 Napoli, Italy
21 Infection and Immunity Division, The Roslin Institute and Royal Dick Schoolof Veterinary Studies, University of

Edinburgh, Easter Bush Veterinary Campus, Edinburgh, EH25 9RG, UK
22 Department of Physiology, Development and Neuroscience, University of Cambridge, Downing Street, Cambridge, CB2 3DY, UK
23 University of Cambridge, Clinical Biochemistry, Addenbrooke's Hospital, Box 232, Hills Road, Cambridge CB2 2QR, UK
24 National Centre of Research 'Frontiers in Genetics', University of Lausanne, Center for Integrative Genomics, BEP, CH-1015 Lausanne, Switzerland
25 University of Manchester, Manchester Heart Centre, Manchester Royal Infirmary, Oxford Road, Manchester M13 9WL, UK
26 University of Manchester, Medical School, Rm 1.302, Stopford Building, University of Manchester, Oxford Road, Manchester, M13 9PT, UK
27 The Wellcome Trust Sanger Institute, Wellcome Trust Genome Campus, Hinxton, Cambridge, CB10 1SA, UK
28 Department of Biochemistry, University of Cambridge, Tennis Court Road, Cambridge, CB2 1GA, UK
29 Department of Statistics, University of Oxford, 1 South Park Road, Oxford, OX1 3TG, UK
30 Department of Genetics, University of Cambridge, Downing Street, Cambridge, CB2 3EH, UK

a Chair of Experimental Genetics, Center of Life and Food Sciences Weihenstephan, Technische Universität München, Ingolstädter Landstr. 1, 85764 Neuherberg, Germany
b Division of Environmental Dermatology and Allergy (UDA), Helmholtz Zentrum München/ Technische Universität München, and Clinical Research Division of Molecular and Clinical Allergotoxicology, Department of Dermatology and Allergy, Technische Universität München, Munich, Germany
c Klinikum der Ludwig-Maximilians-Universität München, Dept. of Neurology, Friedrich-Baur-Institute, Ziemssenstr. 1a, 80336 Munich, Germany
d Heidelberg University Hospital, Im Neuenheimer Feld 410, 69120 Heidelberg, Germany
e Helmholtz Zentrum München, German Research Center for Environmental Health GmbH, Institute of Pathology, Ingolstädter Landstr. 1, 85764 Neuherberg, Germany
f Helmholtz Zentrum München, German Research Center for Environmental Health GmbH, Institute of Human Genetics, Ingolstädter Landstr. 1, 85764 Neuherberg, Germany
g Helmholtz Zentrum München, German Research Center for Environmental Health GmbH, Institute of Lung Biology and Disease, Ingolstädter Landstr. 1, 85764 Neuherberg, Germany
h Technische Universität München, Molecular Nutrional Medicine, Else Kröner-Fresenius Center, Am Forum 8, 85354 Freising-Weihenstephan, Germany
i University of Bonn, Life & Brain Center, Institute of Molecular Psychiatry, Sigmund Freud Str. 25, 53127 Bonn, Germany
j Ludwigs-Maximilians-University München, Gene Center, Institute of Molecular Animal Breeding and Biotechnology, Feodor-Lynen Str. 25, 81377 Munich, Germany
k Chair of Developmental Genetics, Center of Life and Food Sciences Weihenstephan, Technische Universität München, Ingolstädter Landstr. 1, 85764 Neuherberg, Germany